Preprint typeset in JHEP style - HYPER VERSION

LPT Orsay 13-26

The MSSM Higgs sector at a high $\mathrm{M_{SUSY}}$: reopening the low tanβ regime and the search for heavy Higgsses

Abdelhak Djouadi and Jérémie Quevillon

Laboratoire de Physique Théorique, U. Paris XI and CNRS, F–91405 Orsay, France.

Abstract: One of the main implications of the LHC discovery of a Higgs boson with a mass $M_h \approx 126$ GeV is that the scale of supersymmetry–breaking in the Minimal Supersymmetric Standard Model (MSSM) might be rather high, $M_S \gg M_Z$. In this paper, we consider the high M_S regime and study the spectrum of the extended Higgs sector of the MSSM, including the LHC constraints on the mass and the rates of the observed light h state. In particular, we show that in a simplified model that approximates the important radiative corrections, the unknown scale M_S (and some other leading SUSY parameters) can be traded against the measured value of M_h. One would be then essentially left with only two free parameters to describe the Higgs sector, $\tan\beta$ and the pseudoscalar Higgs mass M_A, even at higher orders. The main phenomenological consequence of these high M_S values is to reopen the low $\tan\beta$ region, $\tan\beta \lesssim 3$–5, which was for a long time buried under the LEP constraint on the lightest h mass when a low SUSY scale was assumed. We show that, in this case, the heavier MSSM neutral H/A and charged $H^\pm$ states can be searched for in a variety of interesting final states such as decays into gauge and lighter Higgs bosons (in pairs on in mixed states) and decays into heavy top quarks. Examples of sensitivity on the $[\tan\beta, M_A]$ parameter space at the LHC in these channels are given.

Keywords: Higgs, MSSM, SUSY, LHC.

Contents

1. Introduction

The discovery of a Higgs–like particle by the ATLAS and CMS collaborations [1] in July 2012 was a triumph for the Standard Model (SM) of particle physics as it led to a first verification of one of its cornerstones, the Higgs sector [2–4] that realises the breaking of the electroweak symmetry and generates the masses of the fundamental particle masses. This discovery had also very important consequences on theories beyond the SM, among which supersymmetric theories (SUSY) stood as the most promising ones. This is particularly the case of their minimal low energy realization, the Minimal Supersymmetric Standard

Model (MSSM) [5, 6] in which the electroweak symmetry breaking sector is extended to contain two Higgs doublets which, after symmetry breaking, lead to the existence of five physical states: two CP–even h and H, one CP–odd A and two charged $H^\pm$ bosons [3, 7].

The Higgs observation at the LHC with a mass of approximately 126 GeV first gave support to the MSSM in which the lightest CP–even h boson was predicted to have a mass less than ≈ 130 GeV [8]. An annoying problem is that the measured mass value is too close to the predicted upper limit on M_h in the MSSM, suggesting that the SUSY scale is rather high, $M_S \gtrsim 1$ TeV; see for instance the discussion of Ref. [9]. The fact that M_S is large is backed up by direct SUSY particle searches, which set limits of the order of 1 TeV for the strongly interacting superparticles [10]. In addition, with the precision measurements of its couplings to fermions and gauge bosons, the Higgs state looked more and more SM–like, as no significant deviations from the SM expectation is presently observed [10]. Although this had to be expected since, as is the case in many extended Higgs sectors, there is a decoupling limit [11] in which all the heavier Higgs particles decouple from the SM spectrum and one is left only with the lightest h state which has almost the SM properties, this is again unfortunate. Tests of the properties of the observed Higgs state have to be pursued with more accuracy in order to pin down small deviations from the SM prediction.

An equally important way to probe the MSSM is to search for the direct manifestation of the heavier H, A and $H^\pm$ states. These searches are presently conducted by the ATLAS and CMS collaborations in the regime where $\tan\beta$, the ratio of the vacuum expectations values of the two Higgs fields, is very large, $\tan\beta \equiv v_2/v_1 \gtrsim 5$–10, which significantly enhances the Higgs production rates at the LHC. The regime with low $\tan\beta$, $\tan\beta \lesssim 3$–5, is ignored, the main reason being that if the SUSY scale should not exceed $M_S \approx 3$ TeV to have a still acceptable fine–tuning in the model [12], the h mass is too low and does not match the observed value. More precisely, this $\tan\beta$ region was excluded by the negative Higgs searches that were performed at the ancestor of the LHC, the LEP collider [13].

In this paper, we reopen this low $\tan\beta$ region by simply relaxing the usual assumption that the SUSY scale should be in the vicinity of 1 TeV. In fact, many scenarios with a very large scale M_S have been considered in the recent years, the most popular ones being split–SUSY [14] and high–scale SUSY [15]. In these constructions, the SUSY solution to the hierarchy problem is abandoned and the masses of all the scalars of the theory (and eventually also those of the spin–$\frac{1}{2}$ superparticles in high–scale SUSY) are set to very high values, $M_S \gg M_Z$. Hence, all the sfermions and Higgs bosons are very heavy, except for a light SM–like Higgs boson whose mass can be as low as $M_h \approx 120$ GeV even if $\tan\beta$ is very close to unity. In fact, for this purpose, the scale M_S needs not to be extremely high, for instance close to the unification scale as in the original scenarii of Refs. [14, 15], and values of M_S of order 10 to 100 TeV would be sufficient.

In addition, one may assume that only the sfermions are very heavy and not the Higgs particles, as it is would be the case in non–universal Higgs models where the soft–SUSY breaking mass parameters for the sfermion and the two Higgs doublet fields are disconnected [16]. On would have then a scenario in which the entire MSSM Higgs sector is kept at the electroweak scale, while the sfermions are pushed to the high scale. Such scenarios are also being considered [17] and they might occur in many theoretical constructions.

A first important aspect that we will address in this paper is the treatment of the radiative corrections in the Higgs sector and the derivation of the superparticle and Higgs spectrum in these high scale scenarios. It is well known that for M_S values in the multi–TeV range, the MSSM spectrum cannot be obtained in a reliable way using the usual RGE codes that incorporate the higher order effects [18, 19]: one has first to decouple properly the heavy particles and to resum the large logarithmic contributions. Such a program has been performed in the case where $M_A \approx M_S \gg M_Z$ and the results have been implemented in one of the RGE codes [20]. In the absence of such a tool for $M_S \gg M_A \approx M_Z$ (that is under development [21]), we will adopt the simple approach where the radiative corrections in the Higgs sector are approximated by the dominant contribution in the top and stop sector, which involves the logarithm of the scale M_S and the stop mixing parameter [22]. We will show that, in this approach, the situation simplifies to the extent that one can simply trade the dominant radiative correction against the actual value of the mass of the lighter h boson that has been measured at the LHC to be $M_h \approx 126$ GeV.

One would then deal with a very simple post–h discovery model in which, to a very good approximation, there are only two input parameters in the Higgs sector, M_A and $\tan\beta$ which can take any value (in particular low values $\tan\beta \approx 1$ and $M_A \approx 100$ GeV unless they are excluded by the measurements of the h properties at the LHC) with the mass M_h fixed to its measured value. If one is mainly concerned with the MSSM Higgs sector, this allows to perform rather model–independent studies of this sector.

We should note that while the working approximation for the radiative corrections to Higgs sector is important for the determination of the correct value of M_S (and eventually some other supersymmetric parameters such as the mixing in the stop sector), it has little impact on Higgs phenomenology, i.e. on the MSSM Higgs masses and couplings.

The reopening of the low $\tan\beta$ region allows then to consider a plethora of very interesting Higgs channels to be investigated at the LHC: heavier CP–even H decays into massive gauge bosons $H \to WW, ZZ$ and Higgs bosons $H \to hh$, CP–odd Higgs decays into a vector and a Higgs boson, $A \to hZ$, CP–even and CP–odd Higgs decays into top quarks, $H/A \to t\bar{t}$, and even charged Higgs decay $H^\pm \to Wh$. Many search channels discussed in the context of a heavy SM Higgs boson or for resonances in some non–SUSY beyond the SM (new gauge bosons or Kaluza–Klein excitations) can be used to search for these final states. A detailed discussion of the Higgs cross sections times decay rates in these process is made in this paper and an estimate of the sensitivity that could be achieved at the present $\sqrt{s} = 8$ TeV run with the full data set is given. These processes allow to cover a large part of the parameter space of the MSSM Higgs sector in a model–independent way, i.e. without using the information on the scale M_S and more generally on the SUSY particle spectrum that appear in the radiative corrections.

The rest of the paper is organised as follows. In the next section, we discuss the radiative corrections in the Higgs sector when M_h is used as input and their impact on the Higgs masses and couplings. In section 3, we summarize the various processes for Higgs production and decay in the high and low $\tan\beta$ regions and, in section 4, their implications for the MSSM parameter space. In section 5, we discuss the important new heavy Higgs channels that can be probed at the LHC at low $\tan\beta$. A conclusion is given in section 6.

2. The Higgs sector of the MSSM in the various $\tan\beta$ regimes

In this section, we review the theoretical aspects of the MSSM Higgs sector with some emphasis on the properties of the Higgs particles in the low $\tan\beta$ regime, $1 \lesssim \tan\beta \lesssim 3$, which contrary to the high $\tan\beta$ regime, has not received much attention in the literature.

2.1 The radiatively corrected Higgs masses

Let us begin by recalling a few basics facts about the MSSM and its extended Higgs sector. In the MSSM, two chiral superfields with respective hypercharges -1 and $+1$ are needed for the cancellation of chiral anomalies and their scalar components, the two doublet fields H_1 and H_2, give separately masses to the isospin $-\frac{1}{2}$ and $+\frac{1}{2}$ fermions in a SUSY invariant way. After spontaneous symmetry breaking, the two doublet fields lead to five Higgs particles: two CP–even h, H bosons, a pseudoscalar A boson and two charged $H^\pm$ bosons [3, 7].

The Higgs sector should be in principle described by the four Higgs boson masses and by two mixing angle α and β, with α being the angle which diagonalises the mass matrix of the two CP–even neutral h and H states while β is given in terms of the ratio of vacuum expectation values of the two Higgs fields H_1 and H_2, $\tan\beta = v_2/v_1$. However, by virtue of SUSY, only two parameters are needed to describe the system at tree–level. It is common practice to chose the two basic inputs to be the pseudoscalar mass M_A, expected to lie in the range between M_Z and the SUSY breaking scale M_S, and the ratio $\tan\beta$, which is expected to take values in the range [23]

$$1 \lesssim \tan\beta \lesssim \bar{m}_t/\bar{m}_b \approx 60 \tag{2.1}$$

with $\bar{m}_t$ and $\bar{m}_b$ the running top and bottom quark masses in the $\overline{\rm MS}$ renormalisation scheme evaluated at a scale close to the SUSY scale M_S.

At tree–level, the CP–even h boson mass is then bound to be lighter than the Z boson, $M_h \leq \min(M_Z, M_A)|\cos 2\beta| \leq M_Z$, while the heavier H and $H^\pm$ boson have masses that are comparable to that of the A state if $M_A \gtrsim M_Z$. Likewise, the mixing angle α can be written in compact form in terms of M_A and $\tan\beta$. If the mass M_A is large compared to the Z boson mass, the so called decoupling limit [11] that we will discuss in some detail here, the lighter h state reaches its maximal mass value, $M_h \approx M_Z|\cos 2\beta|$, the heavier CP–even and CP–odd and the charged Higgs states become almost degenerate in mass, $M_H \approx M_A \approx M_{H^\pm}$, while the mixing angle α becomes close to $\alpha \approx \frac{\pi}{2} - \beta$.

As is well known this simple pattern is spoiled when one includes the radiative corrections which have been shown to be extremely important [8, 22, 24–28]. Once these corrections are included, the Higgs masses (and their couplings) will, in principle, depend on all the MSSM parameters. In the phenomenological MSSM (pMSSM) [6], defined by the assumptions that all the soft–SUSY breaking parameters are real with the matrices that eventually describe them being diagonal (and thus, there is no new source of CP or flavor violation) and by the requirement of universal parameters for the first and second generation sfermions, the Higgs sector will depend on, besides M_A and $\tan\beta$, 20 additional parameters: the higgsino mass parameter μ; the bino, wino and gluino mass parameters M_1, M_2, M_3; the first/second and third generation left– and right–handed sfermion mass

parameters $m_{\tilde{q}}, m_{\tilde{u}_R}, m_{\tilde{d}_R}, m_{\tilde{l}}, m_{\tilde{e}_R}$ and $m_{\tilde{Q}}, m_{\tilde{t}_R}, m_{\tilde{b}_R}, m_{\tilde{L}}, m_{\tilde{\tau}_R}$; and finally the (common) first/second and third generation trilinear A_u, A_d, A_e and A_t, A_b, A_τ couplings[1].

Fortunately, only a small subset of these parameters has a significant impact on the radiative corrections to the Higgs sector. At the one loop level, the by far dominant correction to the Higgs masses is originating from top and stop loops and grows like the fourth power of the top quark mass, logarithmically with the stop masses and quadratically with the stop trilinear coupling. The leading component of this correction reads[2] [22]

$$\epsilon = \frac{3\,\bar{m}_t^4}{2\pi^2 v^2 \sin^2\beta}\left[\log\frac{M_S^2}{\bar{m}_t^2} + \frac{X_t^2}{M_S^2}\left(1 - \frac{X_t^2}{12\,M_S^2}\right)\right] \tag{2.2}$$

where $\bar{m}_t$ is again the running $\overline{\rm MS}$ top quark mass to account for the leading two–loop QCD and electroweak corrections in a renormalisation group (RG) improvement (some higher order effects can also be included) [25]. We have defined the SUSY–breaking scale M_S to be the geometric average of the two stop masses $M_S = \sqrt{m_{\tilde{t}_1} m_{\tilde{t}_2}}$; this scale is generally kept in the vicinity of the TeV scale to minimize the amount of fine tuning. We have also introduced the stop mixing parameter $X_t = A_t - \mu \cot\beta$, that we define here in the $\overline{\rm DR}$ scheme, which plays an important role and maximizes the radiative correction when

$$X_t = \sqrt{6}\, M_S \;\; : \;\; \text{maximal mixing scenario} \tag{2.3}$$

while the radiative corrections is smallest for a vanishing X_t value, i.e. in the no mixing scenario $X_t = 0$. An intermediate scenario is when X_t is of the same order as the SUSY scale, $X_t = M_S$, the typical mixing scenario. These scenarios have been often used in the past as benchmarks for MSSM Higgs studies [31] and have been updated recently [32].

The ϵ approximation above allows to write the masses of CP–even Higgs bosons in a particularly simple form

$$M_{h,H}^2 = \frac{1}{2}(M_A^2 + M_Z^2 + \epsilon)\left[1 \mp \sqrt{1 - 4\frac{M_Z^2 M_A^2 \cos^2 2\beta + \epsilon(M_A^2 \sin^2\beta + M_Z^2\cos^2\beta)}{(M_A^2 + M_Z^2 + \epsilon)^2}}\right] \tag{2.4}$$

In this approximation, the charged Higgs mass does not receive radiative corrections, the leading contributions being of $\mathcal{O}(\alpha m_t^2)$ and one can still write the tree-level relation $M_{H^\pm} = \sqrt{M_A^2 + M_W^2}$. For large values of the pseudoscalar Higgs boson mass, the CP–even Higgs masses can be expanded in powers of M_Z^2/M_A^2 to obtain at first order

$$\begin{aligned} M_h^2 &\overset{M_A \gg M_Z}{\to} (M_Z^2\cos^2 2\beta + \epsilon \sin^2\beta)\left[1 + \frac{\epsilon M_Z^2 \cos^2\beta}{M_A^2(M_Z^2 + \epsilon\sin^2\beta)} - \frac{M_Z^2\sin^2\beta + \epsilon\cos^2\beta}{M_A^2}\right] \\ M_H^2 &\overset{M_A \gg M_Z}{\to} M_A^2\left[1 + \frac{M_Z^2\sin^2 2\beta + \epsilon\cos^2\beta}{M_A^2}\right] \end{aligned} \tag{2.5}$$

and indeed, in exact decoupling $M_A/M_Z \to \infty$, one would have $M_H = M_A = M_{H^+}$ for the heavier Higgs states and, for the lighter h boson, the well known relation

$$M_h \equiv M_h^{\rm max} = \sqrt{M_Z^2\cos^2 2\beta + \epsilon \sin^2\beta} \tag{2.6}$$

[1] The first/second generation couplings have no impact in general and can be ignored in practice, reducing the effective number of free inputs of the pMSSM, from 22 to 19 parameters.

[2] Note the typographical error for this equation in Ref. [7] which translated to Refs. [9, 29, 30].

In view of the large value $M_h \approx 126$ GeV of the observed Higgs state at the LHC, it is clear that some optimization of the various terms that enter the mass formula eq. (2.6) with the radiative correction eq. (2.2) is required. As was discussed in many instances including Refs. [9, 29, 30], one needs: *i*) to be close to the decoupling limit $M_A \gg M_Z$ and to have significant $\tan\beta$ values that lead to $|\cos 2\beta| \to 1$ to maximize the tree–level mass and, *ii*) to be in the maximal mixing scenario $X_t = \sqrt{6} M_S$ with the largest possible value of the SUSY–breaking scale M_S to maximize the radiative corrections. As the other SUSY–breaking parameters do not affect significantly the $M_h^{\rm max}$ value, one can fix them to some value. For instance, one can make the choice [32]

$$M_{h\,\rm bench}^{\rm max}: \begin{array}{c} M_2 \simeq 2M_1 = |\mu| = \frac{1}{5} M_S,\; M_3 = m_{\tilde{q}_i} = \frac{1}{3} m_{\tilde{\ell}_i} = 1.5 M_S,\; A_i = 0, \\ m_{\tilde{b}_R} = \frac{1}{3} m_{\tilde{\tau}_i} = M_S\,,\; A_b = A_\tau = A_t \end{array} \tag{2.7}$$

where $m_{\tilde{q}_i}$ and $m_{\tilde{\ell}_i}$ are the common first/second sfermion SUSY–breaking masses and A_i their trilinear couplings. Alternatively, one can perform a scan of these parameters in a reasonable range which should change the resulting value of $M_h^{\rm max}$ in the $\overline{\rm DR}$ scheme only by a few GeV in general.

In the case of a not too large SUSY scale, $M_S \lesssim 3$ TeV, the numerical analyses of the MSSM Higgs sector can be performed with RGE programs [18, 19] such as `Suspect` which include the most relevant higher order radiative corrections in the calculation of the Higgs and superparticle masses (and their couplings). In particular, for the Higgs sector, the full set of one–loop radiative corrections which include also the sbottom and stau loop corrections that are important at high $\tan\beta$ values [24] and the dominant two–loop QCD and electroweak corrections [26] are incorporated in the $\overline{\rm DR}$ scheme; the dominant three–loop corrections are also known [28] but they are quite small and they can be neglected.

One should compare the results with those obtained with the program `FeynHiggs` [33] which incorporates the radiative corrections at the same level of accuracy but in the on–shell renormalisation scheme [27]. In most cases, one obtains comparable results but in some scenarios, the difference in the values of M_h can be as large as 3 GeV. We will thus assume, as in Ref. [32], that there is a $\Delta M_h \approx 3$ GeV uncertainty on the determination of the h mass in the MSSM and that the value $M_h = 126$ GeV of the particle observed at the LHC corresponds to a calculated mass within the pMSSM of

$$123 \text{ GeV} \leq M_h \leq 129 \text{ GeV} \tag{2.8}$$

This uncertainty includes the parametric uncertainties of the SM inputs, in particular the $\overline{\rm MS}$ b–quark mass and the top quark pole mass $\overline{m}_b(m_b) = 4.7$ GeV and $m_t^{\rm pole} = 173.2 \pm 1$ GeV [34]. In the latter case, it is assumed that the top quark mass measured at the Tevatron, with the uncertainty of 1 GeV, is indeed the pole mass. If the top mass is instead extracted from the top pair production cross section, which provides a theoretically less ambiguous determination of $m_t^{\rm pole}$, the uncertainty would be of order 3 GeV [35]. Including also the experimental error in the M_h measurement by ATLAS and CMS, $M_h = 125.7 \pm 0.4$ GeV, the possible calculated mass value of the h boson in the MSSM can be extended to the much wider and admittedly rather conservative range $120 \text{ GeV} \leq M_h \leq 132$ GeV.

2.2 The low $\tan\beta$ regime

The previous discussion assumed a not too high SUSY–breaking scale, $M_S \lesssim 3$ TeV, in order not to have a too large fine-tuning in the model. However, in many scenarios, values of M_S in the 10 TeV range and even beyond have been considered, with a most popular one being the split–SUSY scenario [14, 36]. Indeed, as the criterion to quantify the acceptable amount of tuning is rather subjective, one could well have a very large value of M_S which implies that no sfermion is accessible at the LHC or at any foreseen collider, with the immediate advantage of solving the flavor and CP problems in the MSSM by simply decoupling these states. The mass parameters for the spin–$\frac{1}{2}$ particles, the gauginos and the higgsinos, can be kept close to the electroweak scale, allowing for a solution to the dark matter problem and a successful gauge coupling unification, the two other SUSY virtues. The SUSY solutions to these two remaining problems are abandoned if one takes the very extreme attitude of assuming that the gauginos and higgsinos are also very heavy, with a mass close to the scale M_S, as is the case of the so–called high–scale SUSY models [15, 36].

In all these these SUSY scenarios, there is still a light particle, the h boson, which can have a mass close to 126 GeV for a given choice of parameters such as M_S and $\tan\beta$; see for instance Refs. [9, 36]. The other Higgs particles are much heavier as the pseudoscalar Higgs mass is very often related to the mass scale of the scalar fermions of the theory, $M_A \approx M_S$. However, this needs not to be the case in general, in particular for M_S values not orders of magnitude larger than 1 TeV. Even, in constrained minimal Supergravity–like scenarios, one can assume that the soft SUSY–breaking scalar mass terms are different for the sfermions and for the two Higgs doublets, the so–called non–universal Higgs mass models [16] in which the mass M_A is decoupled from M_S. Scenarios with very large values of M_S and values of M_A close to the weak scale have been advocated in the literature [17], while models in which one of the soft SUSY–breaking Higgs mass parameters, in general M_{H_1}, is at the weak scale while M_S is large are popular; examples are the focus point scenario [37] and the possibility also occurs in M/string theory inspired scenarios [38].

Hence, if one is primarily concerned with the MSSM Higgs sector, one may be rather conservative and assume any value for the pseudoscalar Higgs mass M_A irrespective of the SUSY scale M_S. This is the quite "model–independent" approach that we advocate and will follow in this paper: we take M_A as a free parameter of the pMSSM, with values ranging from slightly above 100 GeV up to order M_S, but make no restriction on the SUSY scale which can be set to any value.

Nevertheless, in scenarios with $M_S \gg 1$ TeV, the Higgs and SUSY mass spectrum cannot be calculated reliably using standard RGE programs as one has to properly decouple the heavy states from the low-energy theory and resum the large logarithmic corrections. A comprehensive study of the split SUSY spectrum has been performed in Ref. [20] and the various features implemented in an adapted version of the code `SuSpect`. However, this version does not include the possibility $M_S \gg M_A \gtrsim M_Z$ that is of interest for us here. A comprehensive and accurate description of the high M_S scenario in the MSSM in the light of the h discovery, including the possibility of a Higgs sector at the weak scale, is under way [21]. In the meantime, we will use the ϵ approximation of eq. (2.2) to describe

the radiative corrections in our high M_S scenario which should be a good approximation for our purpose. In particular, for $M_A \gg M_Z$, we have verified that our results are in a relatively good agreement with those derived in the more refined approach of Ref. [20].

Let us now discuss the magnitude of the SUSY scale that is needed to make small $\tan\beta$ values viable. We make use of the program `Suspect` in which the possibility $M_S \gg 1$ TeV is implemented [20] and which includes the full set of radiative corrections (here we assume the maximal mixing $X_t = \sqrt{6}M_S$ scenario and we take 1 TeV for the gaugino and higgsino masses). In Fig. 1, displayed are the contours in the plane $[\tan\beta, M_S]$ for fixed mass values $M_h = 120, 123, 126, 129$ and 132 GeV of the observed Higgs state (these include the 3 GeV theoretical uncertainty and also a 3 GeV uncertainty on the top quark mass).

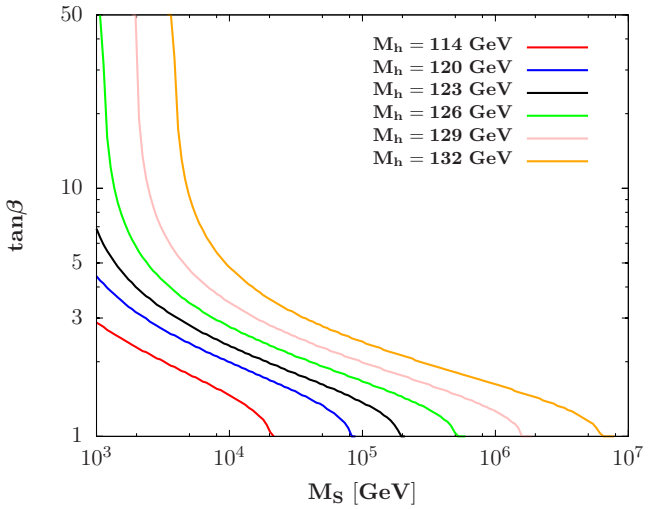

Figure 1: Contours for fixed values $M_h = 120, 123, 126, 129$ and 132 GeV in the $[\tan\beta, M_S]$ plane in the decoupling limit $M_A \gg M_Z$; the "LEP2 contour" for $M_h = 114$ GeV is also shown.

From the figure, one concludes that values of $\tan\beta$ close to unity are possible and allow for an acceptable M_h value provided the scale M_S is large enough. For instance, while one can accommodate a scale $M_S \approx 1$ TeV with $\tan\beta \approx 5$, a large scale $M_S \approx 20$ TeV is required to reach $\tan\beta \approx 2$; to reach the limit $\tan\beta = 1$, an order of magnitude increase of M_S will be needed. Outside the decoupling regime, the obtained M_S for a given M_h value will be of course larger. For completeness, we also show the contour for the mass value $M_h = 114$ GeV, the 95% confidence level limit obtained at LEP2 on a SM–like Higgs boson; it illustrates the fact that values down to $\tan\beta \approx 1$ are still allowed by this bound provided that $M_S \gtrsim 10$ TeV. The implications of this feature will be discussed later.

In the rest of this paper, we will thus consider situations with the MSSM Higgs sector at the weak scale and the only requirement that we impose is that it should be compatible with the LHC data and, in particular, with the mass and production rates of the Higgs boson that has been observed. The requirement that $M_h \approx 126$ GeV, within the theoretical and experimental uncertainties, will be turned into a requirement on the parameters that enter the radiative corrections and, hence, on the scale M_S and the mixing parameter X_t, for given values of the two basics inputs M_A and $\tan\beta$.

2.3 The Higgs couplings and the approach to the decoupling limit

Let us now turn to the important issue of the Higgs couplings to fermions and gauge bosons. These couplings strongly depend on $\tan\beta$ as well as on the angle α (and hence on M_A); normalized to the SM Higgs couplings, they are given in Table 1. The A boson has no tree level couplings to gauge bosons as a result of CP–invariance, and its couplings to down–type and up–type fermions are, respectively, proportional and inversely proportional to $\tan\beta$. This is also the case for the couplings of the charged Higgs boson to fermions, which are admixtures of $\bar{m}_b \tan\beta$ and $\bar{m}_t \cot\beta$ terms and depend only on $\tan\beta$. For the CP–even Higgs bosons h and H, the couplings to fermions are ratios of sines and cosines of the angles α and β; the couplings to down (up) type are enhanced (suppressed) compared to the SM Higgs couplings for $\tan\beta > 1$. The two states share the SM Higgs couplings to vector bosons as they are suppressed by $\sin(\beta-\alpha)$ and $\cos(\beta-\alpha)$, respectively for h and H. We note that there are also couplings between a gauge and two Higgs bosons which in the case of the CP–even states are complementary to those to two gauge bosons $g_{hAZ} \propto g_{hH^+W^-} \propto g_{HVV}$ and vice versa for $h \leftrightarrow H$; the coupling $g_{AH^+W^-}$ has full strength.

Φ	$g_{\Phi\bar{u}u}$	$g_{\Phi\bar{d}d}$	$g_{\Phi VV}$	$g_{\Phi AZ}/g_{\Phi H^+W^-}$
h	$\cos\alpha/\sin\beta$	$-\sin\alpha/\cos\beta$	$\sin(\beta-\alpha)$	$\propto \cos(\beta-\alpha)$
H	$\sin\alpha/\sin\beta$	$\cos\alpha/\cos\beta$	$\cos(\beta-\alpha)$	$\propto \sin(\beta-\alpha)$
A	$\cot\beta$	$\tan\beta$	0	$\propto 0/1$

Table 1: The couplings of the neutral MSSM Higgs bosons, collectively denoted by Φ, to fermions and gauge bosons when normalized to the SM Higgs boson couplings.

These couplings are renormalized essentially by the same radiative corrections that affect the CP–even neutral Higgs masses. In the ϵ approximation discussed above, the one–loop radiatively corrected mixing angle $\bar{\alpha}$ will indeed read

$$\tan 2\bar{\alpha} = \tan 2\beta \, \frac{M_A^2 + M_Z^2}{M_A^2 - M_Z^2 + \epsilon/\cos 2\beta} \; , \qquad -\frac{\pi}{2} \leq \alpha \leq 0 \tag{2.9}$$

This leads to corrected reduced h, H couplings to gauge bosons that are simply $g_{hVV} = \sin(\beta-\bar{\alpha})$ and $g_{HVV} = \cos(\beta-\bar{\alpha})$ and similarly for the couplings to fermions.

The decoupling limit is controlled by the VV coupling of the heavier CP–even Higgs boson, $g_{HVV} = \cos(\beta-\bar{\alpha})$, which vanishes in this case, while the hVV coupling $g^2_{hVV} = 1 - g^2_{HVV} = \sin^2(\beta-\bar{\alpha})$ becomes SM–like. Performing again an expansion in terms of the pseudoscalar Higgs mass, one obtains in the approach to the decoupling limit[3]

$$g_{HVV} \overset{M_A \gg M_Z}{\longrightarrow} \chi \equiv \frac{1}{2}\frac{M_Z^2}{M_A^2} \, \sin 4\beta - \frac{1}{2}\frac{\epsilon}{M_A^2} \, \sin 2\beta \quad \to 0 \tag{2.10}$$

where, in the intermediate step, the first term is due to the tree–level contribution and the second one to the one–loop contribution ϵ. Concentrating first on the tree–level part, one

[3]We thank Nazila Mahmoudi for discussions concerning these limits.

realises that for large values of $\tan\beta$ and also for values very close to unity, the decoupling limit is reached more quickly. Indeed the expansion parameter involves also the factor $\sin 4\beta$ which becomes in these two limiting cases

$$\sin 4\beta = \frac{4\tan\beta(1-\tan^2\beta)}{(1+\tan^2\beta)^2} \to \begin{cases} -4/\tan\beta & \text{for } \tan\beta \gg 1 \\ 1-\tan^2\beta & \text{for } \tan\beta \sim 1 \end{cases} \to 0 \tag{2.11}$$

Hence, in both the $\tan\beta \gg 1$ and $\tan\beta \sim 1$ cases, the g_{HVV} coupling that controls the decoupling limit $M_Z^2/M_A^2 \to 0$, is doubly suppressed. The radiatively generated component, if one recalls that the one–loop correction in eq. (2.2) involves a $1/\sin^2\beta$ term which makes it behave as $-\epsilon/M_A^2 \times \cot\beta$, also vanishes at high $\tan\beta$ values. This leads to the well known fact that the decoupling limit $g_{HVV} \to 0$ is reached very quickly in this case, in fact as soon as $M_A \gtrsim M_h^{\rm max}$. Instead, for $\tan\beta \approx 1$, this radiatively generated component is maximal. However, when both components are included, the departure from the decoupling limit in the coupling g_{HVV} for a fixed M_A value occurs when $\sin 4\beta \approx -1$, which corresponds to $\beta = 3\pi/8$ and hence to the value $\tan\beta \approx 2.4$.

Similarly to the HVV case, one can write the couplings of the CP–even Higgs states to isospin $\frac{1}{2}$ and $-\frac{1}{2}$ fermions in the approach to the decoupling limit $M_Z^2/M_A^2 \ll 1$ as

$$\begin{aligned} g_{huu} &\overset{M_A \gg M_Z}{\longrightarrow} 1 + \chi\ \cot\beta &&\to 1 \\ g_{hdd} &\overset{M_A \gg M_Z}{\longrightarrow} 1 - \chi\ \tan\beta &&\to 1 \\ g_{Huu} &\overset{M_A \gg M_Z}{\longrightarrow} -\cot\beta + \chi &&\to -\cot\beta \\ g_{Hdd} &\overset{M_A \gg M_Z}{\longrightarrow} +\tan\beta + \chi &&\to +\tan\beta \end{aligned}$$

with the expansion parameter $\chi \propto 1/M_A^2$ is the same as the one given in eq. (2.10). In the $M_A \gg M_Z$ regime, the couplings of the h boson approach those of the SM Higgs boson, $g_{huu} \approx g_{hdd} \approx 1$, while the couplings of the H boson reduce, up to a sign, to those of the pseudoscalar Higgs boson, $g_{Huu} \approx g_{Auu} = \cot\beta$ and $g_{Hdd} \approx g_{Add} = \tan\beta$. Again, as a result of the presence of the same combination of $M_Z^2 \sin 4\beta$ and $\epsilon \sin 2\beta$ factors in the expansion term χ of all couplings, the limiting values are reached more quickly at large values of $\tan\beta$ but the departure from these values is slower at low $\tan\beta$.

In Fig. 2, we display the square of the H couplings to gauge bosons and fermions as a function of $\tan\beta$ for $M_A = 300$ GeV. Again the maximal mixing scenario is assumed and M_S is chosen in such way that for any $\tan\beta$ value, one has $M_h = 126$ GeV. At such A masses, the couplings of the lighter h boson to all particles deviate little from unity even for small $\tan\beta$ values and in this case too one can consider that we are already in the decoupling regime. Nevertheless, the coupling of the heavier H boson to VV states is still non–zero, in particular at low $\tan\beta$. The H coupling to $t\bar{t}$ pairs states (as well as the A coupling) is significant at low $\tan\beta$ values, $g_{Htt}^2 \gtrsim 0.1$ for $\tan\beta \lesssim 3$.

This demonstrates that the heavier $H/A/H^\pm$ bosons can have sizable couplings to top quarks (and to massive gauge bosons for H outside the decoupling regime) if $\tan\beta$ values as low as $\tan\beta \sim 3$ are allowed. In fact, the $H/A/H^\pm$ couplings to top quarks $\propto \cot\beta$ are larger that the couplings to bottom quarks $\propto \tan\beta$ for values $\tan\beta \approx \sqrt{\bar{m}_t/\bar{m}_b} \lesssim 7$ and this value should be considered as the boundary between the high and low $\tan\beta$ regimes. With

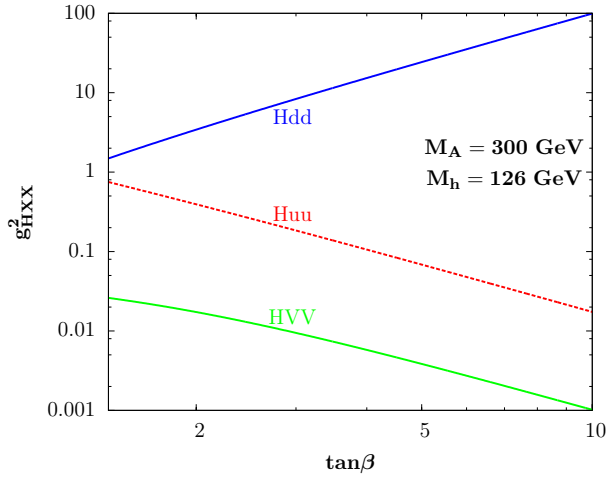

Figure 2: The squared couplings of the heavier CP–even H state to gauge bosons and fermions as a function of $\tan\beta$ for $M_A = 300$ GeV. The SUSY scale is chosen so that $M_h = 126$ GeV.

more refinement, one can consider three $\tan\beta$ regimes: the high regime with $\tan\beta \gtrsim 10$, the intermediate regime with $5 \lesssim \tan\beta \lesssim 10$ and the low regime with $\tan\beta \lesssim 5$.

There are two important remarks which should be made before closing this section. The first one is that besides the ϵ correction, there are additional one–loop vertex corrections which modify the tree–level Higgs–fermion couplings [39]. In the case of b–quarks in the high (and eventually intermediate) $\tan\beta$ regime, they can be very large in the b–quark case as they grow as $\bar{m}_b \tan\beta$. The dominant component comes from the SUSY–QCD corrections with sbottom–gluino loops that can be approximated by

$$\Delta_b \simeq \frac{2\alpha_s}{3\pi}\mu m_{\tilde{g}} \tan\beta / \max(m^2_{\tilde{g}}, m^2_{\tilde{b}_1}, m^2_{\tilde{b}_2}) \tag{2.12}$$

In the decoupling limit $M_A \gg M_Z$, the reduced $b\bar{b}$ couplings of the H, A states read

$$g_{Hbb} \approx g_{Abb} \approx \tan\beta \left[1 - \frac{\Delta_b}{1+\Delta_b}\right] \tag{2.13}$$

In the case of the lighter h boson, the hbb couplings stay SM–like in this limit in principle, but slightly outside the decoupling limit, there is a combination of SUSY parameters which realises the so–called "vanishing coupling" regime [31] in which $\bar{\alpha} \to 0$ and hence $g_{hbb} \ll 1$.

The second remark concerns the trilinear Hhh coupling which will be needed in our analysis. In units of M_Z^2/v, this coupling is given at tree–level by [3]

$$\lambda_{Hhh} \approx 2\sin 2\alpha \sin(\beta+\alpha) - \cos 2\alpha \cos(\beta+\alpha) \tag{2.14}$$

Again, to include the radiative corrections in the ϵ approximation, one needs to perform the change $\alpha \to \bar{\alpha}$; however, in this case, there are also direct vertex corrections but they can be still described by the ϵ parameter. One obtains in this approach [40]

$$\lambda_{Hhh} \overset{M_A \gg M_Z}{\longrightarrow} -\frac{3}{M_Z^2}\left[\sqrt{(M_h^2 - \epsilon\sin^2\beta)(M_Z^2 - M_h^2 + \epsilon\sin^2\beta)} + \epsilon \sin\beta\cos\beta\right] \tag{2.15}$$

At high–$\tan\beta$, the trilinear coupling vanishes $\lambda_{Hhh} \to 0$ while for small and intermediate $\tan\beta$ values it stays quite substantial as a result of the large ϵ corrections.

3. Higgs decays and production at the LHC

3.1 The high and intermediate $\tan\beta$ regimes

The production and decay pattern of the MSSM Higgs bosons crucially depend on $\tan\beta$. In the LHC run up to now, i.e. with center of mass energies up to $\sqrt{s} = 8$ TeV, only relatively large $\tan\beta$ values, $\tan\beta \gtrsim 5$–10 which correspond to the high and intermediate regimes, are probed in the search of the neutral H/A and the charged $H^\pm$ bosons. In the high $\tan\beta$ regime, the couplings of these non–SM like Higgs bosons to b quarks and to τ leptons are so strongly enhanced, and the couplings to top quarks and massive gauge bosons so suppressed, that the pattern becomes rather simple.

A first simplifying feature is that the decoupling regime in which the lighter h boson attains its maximal mass $M_h^{\rm max}$ value for a given SUSY parameter set[4] and has SM–couplings is reached already at $M_A \gtrsim M_h^{\rm max}$ for $\tan\beta \gtrsim 10$. In this case, the heavier CP–even H boson has approximately the same mass as the A boson and its interactions are similar. Hence, the spectrum will consist of a SM–like Higgs $h \equiv H_{\rm SM}$ and two pseudoscalar (like) Higgs particles, $\Phi = H/A$. The $H^\pm$ boson will also be approximately degenerate in mass with the Φ states and the intensity of its couplings to fermions will be similar.

An immediate consequence will be that the h boson will precisely decay into the variety of final states and will be produced in the various channels that are present in the SM. These decay and production processes have been studied in detail at various places, see Ref. [4] for a detailed review and Refs. [42, 44] for updates. We will discuss the implications of these channels for the properties of the state observed at the LHC in the next section.

In the case of the heavier neutral $\Phi = H/A$ bosons, the decay pattern is very simple: the $t\bar{t}$ channel and all other decay modes are suppressed to a level where their branching ratios are negligible and the Φ states decay almost exclusively into $\tau^+\tau^-$ and $b\bar{b}$ pairs, with branching ratios of ${\rm BR}(\Phi \to \tau^+\tau^-) \approx m_\tau^2/[3\overline{m}_b^2(M_\Phi)+m_\tau^2] \approx 10\%$ and ${\rm BR}(\Phi \to b\bar{b}) \approx 90\%$. The charged Higgs particles decay into $H^\pm \to \tau\nu_\tau$ final states with a branching fraction of almost 100% for $H^\pm$ masses below the tb threshold, $M_{H^\pm} \gtrsim m_t + m_b$, and a branching ratio of only $\approx 10\%$ for masses above this threshold. The by far dominant channel in the latter case is $H^\pm \to tb$ which occurs with a $\approx 90\%$ probability for the same reason as above.

Concerning Higgs production in the high $\tan\beta$ regime, the enhancement of the b–quark couplings makes that only processes involving this quark are important for the $\Phi = H/A$ states. In the dominant gluon fusion production channel. $gg \to \Phi$, one should take into account the b–quark loop which provides the largest contribution (in contrast to the SM where the top quark contribution largely dominates) and in associated Higgs production with heavy quarks, $b\bar{b}$ final states and hence the processes $gg/q\bar{q} \to b\bar{b} + \Phi$, must be

[4]The present discussion holds in the case where the h boson is the SM–like state which implies $M_A \gtrsim M_h^{\rm max}$. At low M_A values, the role of the CP–even h and H states are reversed: it is H which is the SM–like particle $H \equiv H_{\rm SM}$ and h would correspond to the pseudoscalar–like Higgs particle. However, the possibility that the H state is the observed particle at the LHC is ruled out by present data [30]. A special case would be $M_A \approx M_h^{\rm max}$, which is called the intense coupling regime in Ref. [41] and which leads to mass degenerate h, H, A states with comparable couplings to fermions; as the h and H states are close in mass, one has the same phenomenology as in the decoupling limit where H has the same properties as A [42, 43]. Again, this scenario is strongly disfavored by present data [30].

considered. The latter processes are equivalent to the $b\bar{b} \to \Phi$ channels when no–additional b–quark in the final state is present, if one considers the b–quark as a massless parton and uses heavy quark distribution functions in a five active flavor scheme [45].

Hence, except for the $gg \to \Phi$ and $b\bar{b} \to \Phi$ fusion processes, all the other production channels are irrelevant in the high $\tan\beta$ regime, in particular the vector boson fusion and the Higgs–strahlung channels, that are absent for A and strongly suppressed for H. In both cases, as $M_\Phi \gg m_b$, chiral symmetry holds and the cross sections are approximately the same for the CP–even H and CP–odd A bosons. The cross section for $gg \to \Phi$ is known up to next–to–leading order in QCD [46] and can be calculated using the program `HIGLU` [47, 48]. The $bb \to \Phi$ rate is instead known up to NNLO in QCD [49, 50] and its evaluation can be made using the programs `bb@nnlo` or `SUSHI` [51]. Note that for associated H/A production with two tagged b–quarks in the final states that can be used, one should instead consider the process $gg/q\bar{q} \to bb + \Phi$ which is known up to NLO QCD [52]; they leading order cross section can be obtained using the program `QQH` [48].

The most powerful search channel for the heavier MSSM Higgs particles at the LHC is by far the process

$$pp \to gg + b\bar{b} \to \Phi \to \tau^+\tau^- \tag{3.1}$$

The precise values of the cross section times branching fraction for this process at the LHC have been recently updated in Refs. [42, 44] and an assessment of the associated theoretical uncertainties has been made. It turns out that these uncertainties are not that small. They consist mainly of the scale uncertainties due to the missing higher orders in perturbation theory and of the combined uncertainty from the parton distribution functions and the strong coupling constant α_s. When combined, they lead to a total theoretical uncertainty of 20–30% in both the $gg \to \Phi$ and $b\bar{b} \to \Phi$ channels[5]. We will assume here for the combined $gg + b\bar{b} \to \Phi$ channel a theoretical uncertainty of

$$\Delta^{\rm TH}\sigma(pp \to \Phi) \times {\rm BR}(\Phi \to \tau\tau) = \pm 25\% \tag{3.2}$$

in the entire M_Φ range probed at the LHC and for both $\sqrt{s} = 8$ and 14 TeV.

Besides the QCD uncertainty, three other features could alter the rate $\sigma(pp \to \Phi \to \tau\tau)$ in the MSSM and they are related to the impact of the SUSY particle contributions. We briefly summarise them below and some discussions are also given in Refs. [30, 53].

While the CP–odd A state does not couple to identical squarks as a result of CP–invariance, there is a $H\tilde{q}_i\tilde{q}_i$ coupling in the case of the H state which allows squarks, and mainly top and bottom squarks, to contribute to the $gg \to H$ amplitude at leading order (there are NLO contributions [54] for both the Hgg and Agg amplitudes via gluino exchange but they should be smaller). However, as squarks do not couple to the Higgs bosons proportionally to their masses, these contributions are damped by powers of $\tilde{m}_Q^2$

[5] It was advocated in Refs. [42, 43] that there are two additional sources of uncertainties related to the b–quark mass which should be considered: the one in the $gg \to \Phi$ process due to the choice of the renormalization scheme for m_b and the parametric uncertainty. These will increase the total uncertainty. We will however, ignore this complication and retain the "official" estimate of the error given in Ref. [44].

for $M_H \lesssim 2m_Q^2$ and, at high $\tan\beta$. the b–loop contribution stays largely dominant. These SUSY contributions are thus expected to be small and can be neglected in most cases.

A more important effect of the SUSY sector is due to the one–loop vertex correction to the $\Phi b\bar{b}$ couplings, Δ_b of eqs. (2.12–2.13), which can be large in the high $\tan\beta$ regime as discussed previously. However, in the case of the full process $pp \to \Phi \to \tau^+\tau^-$, this correction appears in both the cross section, $\sigma(\Phi) \propto (1+\Delta_b)^{-2}$, and in the branching fraction, $\text{BR}(\tau\tau) = \Gamma(\Phi \to \tau\tau)/[(1+\Delta_b)^{-2}\Gamma(\Phi \to b\bar{b}) + \Gamma(\Phi \to \tau\tau)]$, which involves the Δ_b correction above in the denominator. Hence, in the cross section times branching ratio, the Δ_b corrections largely cancels out and for $\text{BR}(\tau\tau) \approx 10\%$, one obtains

$$\sigma(gg + b\bar{b} \to \Phi) \times \text{BR}(\Phi \to \tau\tau) \approx \sigma \times \text{BR} \times (1 - \frac{1}{5}\Delta_b) \tag{3.3}$$

Hence, one needs a very large Δ_b term (which, one should recall, is a radiative correction), of order unity or more, in order to alter significantly the $pp \to \Phi \to \tau\tau$ rate[6].

Finally, there is the possibility that there are light SUSY particles with masses $\widetilde{m} \lesssim \frac{1}{2}M_\Phi$ which lead to the opening of SUSY decay channels for the H/A states that might reduce the $\Phi \to \tau\tau$ branching fraction. For $M_\Phi \lesssim 1$ TeV, the only possibilities for these superparticles seem to be light neutralinos and charginos (χ) and light sleptons ($\widetilde{\ell}$). These decays have been reviewed in Ref. [7] and they have been found to be in general disfavored in the high $\tan\beta$ regime as the $\Phi \to b\bar{b} + \tau\tau$ decays are so strongly enhanced that they leave little room for other possibilities. Only in a few special situations that these SUSY decays can be significant. For the decays $\Phi \to \chi\chi$, it is the case when i) all $\chi = \chi^\pm_{1,2}$ and $\chi^0_{1\text{–}4}$ channels are kinematically open or ii) if only a subset of χ particles is light, they should be mixtures of gauginos and higgsinos to maximize the $\Phi\chi\chi$ couplings. Both scenarios should be challenged by the present LHC constraints[7]. In the case of sleptons, only the decays into light $\tilde{\tau}$ states could be important; while the decay $A \to \tilde{\tau}_1\tilde{\tau}_1$ is forbidden by CP–invariance, the decays $H \to \tilde{\tau}_1\tilde{\tau}_1$ and $H/A \to \tilde{\tau}_1\tilde{\tau}_2$ can have substantial rates at high $\tan\beta$ when the $\Phi\tilde{\tau}\tilde{\tau}$ coupling is enhanced. However, again, at these large $\tan\beta$ values, the $\Phi \to b\bar{b}$ and $\Phi \to \tau\tau$ decays are extremely enhanced and leave little room for competition.

Thus, only in the unlikely cases where the decay $H \to \tilde{\tau}_1\tilde{\tau}_1$ has a branching rate of the order of 50%, the squark loop contribution to the $gg \to H$ process is of the order 50%, or the Δ_b SUSY correction is larger than 100%, that one can change the $pp \to \Phi \to \tau\tau$ rate by $\approx 25\%$, which is the level of the QCD uncertainty. One thus expects $\sigma(pp \to \Phi) \times \text{BR}(\Phi \to \tau\tau)$ to be extremely robust and to depend almost exclusively on M_A and $\tan\beta$.

Two more processes are considered for the heavier MSSM neutral Higgs bosons at high $\tan\beta$. The first one is $pp \to \Phi \to \mu^+\mu^-$ for which the rate is simply $\sigma(pp \to \Phi \to \tau\tau)$

[6] In any case, if one insists to take this Δ_b correction into account in the constraint on the $[\tan\beta, M_A]$ plane that is obtained from the $pp \to \Phi \to \tau\tau$ rate, one could simply replace $\tan\beta$ by $\tan\beta/(1+\Delta_b/10)$. A contribution $\Delta_b \approx 1$ will change the limit on $\tan\beta$ by only 10%, i.e. less than the QCD uncertainty.

[7] The searches of charginos and neutralinos in the same-sign lepton and tri-lepton topologies at the LHC are now probing significant portions of the gaugino–higgsino parameter space and they exclude more and more the possibility of light χ states [55]. This is particularly true for mixed gaugino–higgsino states in which the $\Phi\chi\chi$ couplings are maximised: the lead to a large gap between the lightest and the next-to-lightest χ masses and hence a large amount of missing energy that make the searches more effective.

rescaled by $\text{BR}(\Phi \to \mu\mu)/\text{BR}(\Phi \to \tau\tau) = m_\mu^2/m_\tau^2 \approx 4 \times 10^{-3}$. The rate is much smaller than in the $\tau\tau$ case and is not compensated by the much cleaner $\mu\mu$ final state and the better resolution on the invariant mass. Searches in this channel have been performed in the SM Higgs case [56] and the sensitivity is very low. In addition, there is the process in which the H/A bosons are produced in association with two b–quark jets and decay into $b\bar{b}$ final states and searches in this channel have been performed by the CMS collaboration with the 7 TeV data [57]. However, the sensitivity is far lower than in the $\tau^+\tau^-$ channel.

Thus, the $pp \to \Phi \to \tau^+\tau^-$ search for the neutral Higgs bosons provides the most stringent limits on the MSSM parameter space at large $\tan\beta$ and all other channels are weaker in comparison and provide only cross checks. We will thus concentrate on this process in the rest of our discussion of the high $\tan\beta$ regime.

A final remark needs to be made on the charged Higgs boson. The dominant $H^\pm$ search channel at present energies is in $H^\pm \to \tau\nu$ final states with the $H^\pm$ bosons produced in top quark decays for masses not too close to $M_{H^\pm} = m_t - m_b \approx 170$ GeV

$$pp \to t\bar{t} \;\text{ with }\; t \to H^+ b \to \tau\nu\, b \tag{3.4}$$

This is particularly true at high $\tan\beta$ values when the $t \to H^+ b$ branching ratio which grows with $\bar{m}_b^2 \tan^2\beta$, is significant. For higher $H^\pm$ masses, one should rely on the three–body production process $pp \to tbH^\pm \to tb\tau\nu$ which leads to a cross section that is also proportional to $\tan^2\beta$, but the rates are presently too small. Hence, processes beyond $t \to bH^+$ can be considered only at the upgraded LHC.

3.2 The low $\tan\beta$ regime

The phenomenology of the heavy MSSM $A, H, H^\pm$ bosons is richer at low $\tan\beta$ and leads to a production and decay pattern that is slightly more involved than in the high $\tan\beta$ regime. Starting with the production cross sections, we display in Fig. 3 the rates for the relevant $H/A/H^\pm$ production processes at the LHC with center of mass energies of $\sqrt{s} = 8$ TeV and $\sqrt{s} = 14$ GeV assuming $\tan\beta = 2.5$. The programs `HIGLU` [47], `SUSHI` [51] and those of Ref. [48] have been used with a calling file in which the radiative corrections in the Higgs sector are calculated according to section 2.1 and lead to a fixed $M_h = 126$ GeV value. The MSTW set of parton distribution functions (PDFs) [58] has been adopted. For smaller $\tan\beta$ values, the cross sections for the various processes, except for $pp \to H/A + b\bar{b}$, are even larger as the H/A couplings to top quarks and the HVV coupling outside the decoupling limit are less suppressed.

Because of CP invariance which forbids AVV couplings, the pseudoscalar state A cannot be produced in the Higgs-strahlung and vector boson fusion processes. For $M_A \gtrsim 300$ GeV, the rate for the associated $pp \to t\bar{t}A$ process is rather small, as is also the case of the $pp \to b\bar{b}A$ cross section which is not sufficiently enhanced by the $Abb \propto \tan\beta$ coupling. Hence, only the $gg \to A$ fusion process with the dominant t–quark and sub-dominant b–quark loop contributions included provides large rates at low $\tan\beta$.

The situation is approximately the same for the CP–even H boson: only the $gg \to H$ process provides significant production rates at relatively high values of M_H, $M_H \gtrsim 300$

GeV, and low $\tan\beta$, $\tan\beta \lesssim 5$. As in the case of A, the cross section for $pp \to t\bar{t}H$ is suppressed compared to the SM case while the rate for $pp \to b\bar{b}H$ is not enough enhanced. However, in this case, the vector boson fusion $pp \to Hqq$ and Higgs-strahlung processes $q\bar{q} \to HW/HZ$ are also at work and have production rates that are not too suppressed compared to the SM at sufficiently low M_H values, $M_H \lesssim 200$–300 GeV and $\tan\beta \approx 1$.

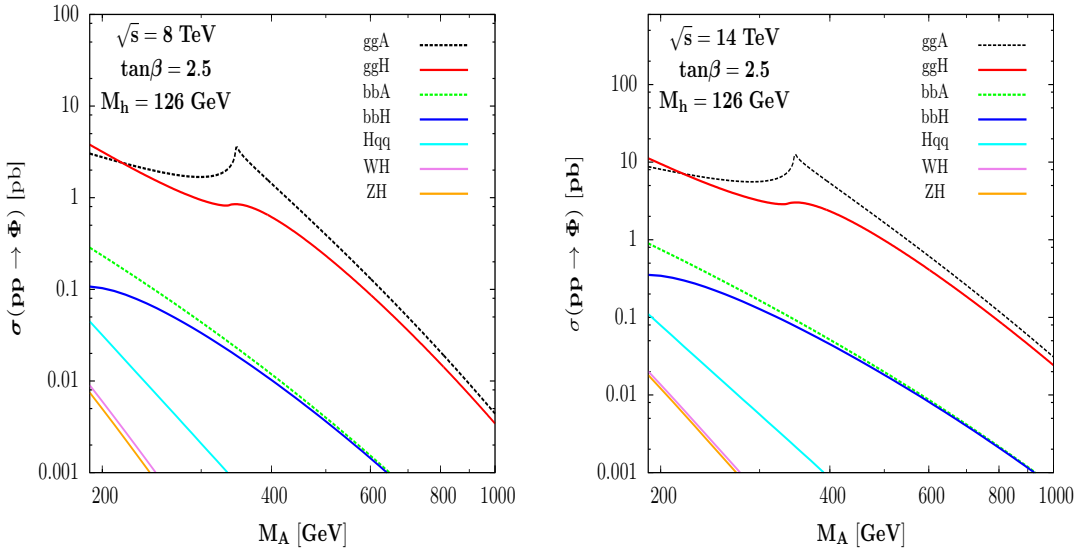

Figure 3: The production cross sections of the MSSM heavier Higgs bosons at the LHC with $\sqrt{s} = 8$ TeV (left) and $\sqrt{s} = 14$ TeV (right) for $\tan\beta = 2.5$. Only the main channels are presented. The higher order corrections are included (see text) and the MSTW PDFs have been adopted.

Hence, for $M_A \gtrsim 300$ GeV, the only relevant production process is $gg \to \Phi$ with the dominant contribution provided by the heavy top quark loop. In this case, one can include not only the large NLO QCD corrections [59], which are known in the exact case [46], but also the NNLO QCD corrections [60] calculated in a effective approach with $m_t \gg M_\Phi$ which should work in practice for $M_\Phi \lesssim 300$ GeV but can be extended to higher masses.

For the charged Higgs boson, the dominant production channel in the low $\tan\beta$ regime is again top quark decays, $t \to H^+b$, for $M_{H^\pm} \lesssim 170$ GeV. Indeed, for $\tan\beta \lesssim 5$, the $m_t/\tan\beta$ component of the $H^\pm tb$ coupling becomes rather large, leading to a significant $t \to H^+b$ branching ratio. For higher $H^\pm$ masses, the main process to be considered is $gg/q\bar{q} \to H^\pm tb$ [61]. As in the case of $pp \to b\bar{b}\Phi$, one can take the b–quark as a parton and consider the equivalent but simpler $2 \to 2$ channel $gb \to H^\pm t$. One obtains an accurate description of the cross section if the renormalisation and factorisation scales are chosen to be low, $\mu_R = \mu_F \approx \frac{1}{6}(M_{H^\pm} + m_t)$ in order to account for the large NLO QCD corrections [62]; the scales uncertainties are large though, being of order 20% [44]. Additional sources of $H^\pm$ states for $M_{H^\pm} \lesssim 250$ GeV are provided by pair and associated production with neutral Higgs bosons in $q\bar{q}$ annihilation as well as H^+H^- pair and associated $H^\pm W^\mp$ production in gg and/or $b\bar{b}$ fusion but the rates are very small [63].

Let us turn to the decay pattern of the heavier MSSM Higgs particles which can be rather involved in the low $\tan\beta$ regime. In this case, as the couplings of the H/A bosons

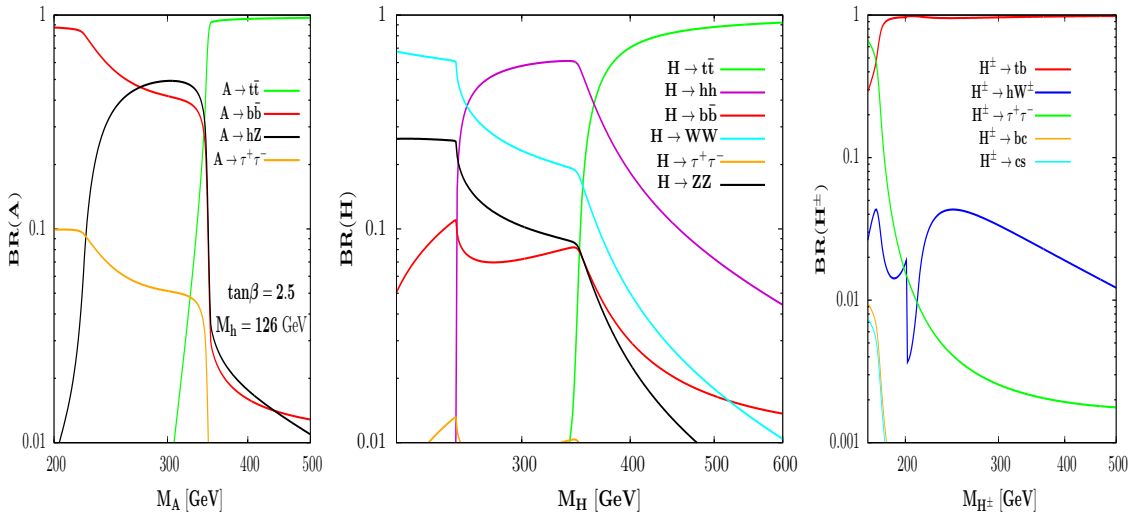

Figure 4: The decay branching ratios of the heavier MSSM Higgs bosons A (left), H (center) and $H^\pm$ (right) as a function of their masses for $\tan\beta = 2.5$. The program `HDECAY` [64] has been used with modifications so that the radiative corrections lead to $M_h = 126$ GeV.

to b–quarks are not very strongly enhanced and the couplings to top quarks (and gauge bosons in the case of the H state) not too suppressed, many interesting channels appear. The branching fractions for the $H/A/H^\pm$ decays are shown in Fig. 4 as functions of their masses at $\tan\beta = 2.5$. They have been obtained using the program `HDECAY` [64] assuming large M_S values and the maximal mixing scenario that lead to a fixed $M_h = 126$ GeV value. The pattern does not significantly depend on other SUSY parameters, provided that Higgs decays into supersymmetric particles are kinematically closed as will be implicitly assumed in the following[8], where the main features of the decays are summarised in a few points.

– Sufficiently above the $t\bar{t}$ threshold for the neutral and the tb threshold for the charged Higgs bosons, the decay channels $H/A \to t\bar{t}$ and $H^+ \to t\bar{b}$ become by far dominant for $\tan\beta \lesssim 3$ and do not leave space for any other decay mode. Note that these decays have also significant branching fractions below the respective kinematical thresholds [65]. It is especially true for the charged Higgs state for which $\text{BR}(H^+ \to t\bar{b}) \gtrsim 1\%$ for $M_{H^\pm} \approx 130$ GeV.

– Below the $t\bar{t}$ threshold, the H boson can still decay into gauge bosons $H \to WW$ and ZZ with rather substantial rates as the HVV couplings are not completely suppressed.

– In the window $2M_h \lesssim M_H \lesssim 2m_t$, the dominant decay mode for $\tan\beta \lesssim 3$ turns out to be the very interesting channel $H \to hh$ channel. As discussed earlier, the Hhh self–couplings given in eq. (2.15) is significant at low $\tan\beta$ values.

– If allowed kinematically, i.e. for $M_A \gtrsim M_h + M_Z$ GeV, the CP–odd Higgs boson can also decay into hZ final states with a significant rate below the $t\bar{t}$ threshold as the AZh coupling (that is the same as the HVV coupling) is substantial. Nevertheless, the $A \to \tau\tau$ channel is still important as it has a branching fraction above $\approx 5\%$ up to $M_A \approx 2m_t$.

[8] In fact, even in this low $\tan\beta$ case, the $t\bar{t}$ decays for sufficiently large masses are so dominant that they do not lead to any significant quantitative change if SUSY particles are light. In addition, being not enhanced by $\tan\beta$, the Δ_b correction has no impact in this low $\tan\beta$ regime.

– In the case of the charged Higgs state, there is also the channel $H^+ \to Wh$ which is important similarly to the $A \to hZ$ case. Note that for $M_{H^\pm} \lesssim 170$ GeV, the decay $H^+ \to c\bar{s}$ that is usually considered only in two–Higgs doublet models and the very interesting flavor changing mode $H^+ \to c\bar{b}$ have rates that are at the percent level. All these exotic channels have larger branching ratios, above $\approx 10\%$, for $\tan\beta$ values close to unity.

3.3 The case of the h boson

A final word is due to the production and decay rates of the lighter h boson that we will assume to be the state with a 126 GeV mass observed at the LHC.

In the left–hand side of Fig. 5, we display the cross sections for the relevant Higgs production channels at the LHC with $\sqrt{s} = 8$ TeV as a function of M_A at $\tan\beta = 2.5$. Again, the radiative corrections in the ϵ approach are such that M_h is fixed to 126 GeV. Shown are the rates for the gluon fusion $gg \to h$, vector boson fusion $qq \to Hqq$, Higgs–strahlung $q\bar{q} \to hW, hZ$ as well as associated $pp \to t\bar{t}h$ processes. The relevant higher order QCD corrections are implemented and the MSTW set of PDFs has been adopted. The rates can be very different whether one is in the decoupling limit $M_A \approx 1$ TeV where the h couplings are SM–like or at low M_A values when the h couplings are modified.

The variation of the branching ratios compared to their SM values, which correspond to their MSSM values in the decoupling limit, are displayed as a function of M_A for $\tan\beta = 2.5$ in the right-hand side of the figure. Sown are the branching fractions for the decays that are currently used to search for the SM Higgs boson, i.e. the channels $h \to bb, \tau\tau, ZZ, WW, \gamma\gamma$. Again, large differences compared to the SM can occur at low to moderate M_A values.

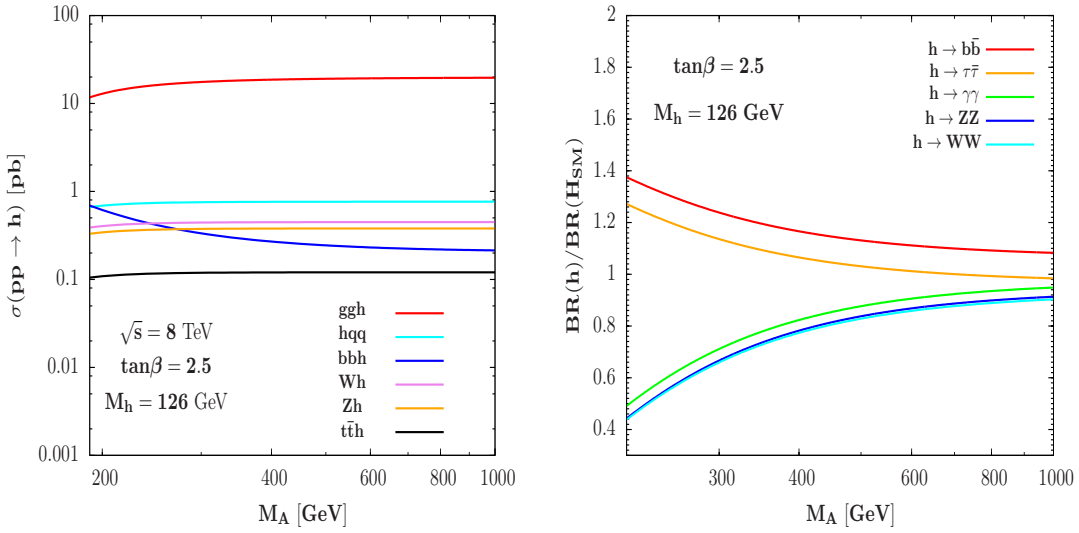

Figure 5: The production cross sections of the lighter h boson at the LHC with $\sqrt{s} = 8$ TeV (left) and the variation of its decay branching fractions compared to the SM values (right) for $\tan\beta = 2.5$. Again, the radiative corrections in the Higgs sector are such that $M_h = 126$ GeV.

The data collected so far by the ATLAS and CMS collaborations on the observed 126 GeV Higgs particle should thus put strong constraints on the parameters $\tan\beta$ and M_A.

4. Present constraints on the MSSM parameter space

4.1 Constraints from the h boson mass and rates

We start this section by discussing the impact of the large amount of ATLAS and CMS data for the observed Higgs state at the LHC on the MSSM parameter space. We will assume for definiteness that the h boson is indeed the observed particle as the possibility that it is the H state instead is ruled out by the LHC data [30].

A first constraint comes from the measured mass of the observed state, $M_h \approx 126$ GeV. As discussed previously and in several other instances such as Ref. [9], in the phenomenological MSSM, this large M_h value indicates that the radiative corrections in the Higgs sector are maximised. If the scale M_S is close to 1 TeV as dictated by naturalness arguments, this implies that one is in the decoupling regime (and hence, dealing with a SM–like Higgs particle) with intermediate to high–$\tan\beta$ values and maximal stop mixing. If the SUSY scale is pushed to $M_S \approx 3$ TeV, the highest acceptable value from fine-tuning adopted in many analyses such that of Refs. [29, 30], a smaller mixing in the Higgs sector and values of M_A of order of a few hundred GeV can be made possible. However, $\tan\beta$ values in the low regime, $\tan\beta \lesssim 3$–5 cannot be accommodated as they lead to $M_h \lesssim 123$ GeV and even to $M_h \lesssim 120$ GeV, which is the lowest value that can be reached when including the theoretical and the top-quark mass uncertainties in the calculation of M_h.

To obtain an acceptable value of M_h in the low $\tan\beta$ regime, one needs to push M_S to the 10 TeV domain or higher. In the approach that we are advocating here, in which the radiative corrections in the MSSM Higgs sector are implemented in the rather simple (but not completely inaccurate) approximation where only the leading RGE improved one–loop correction of eq. (2.2) is taken into account, one can trade the (unknown) values of M_S and the mixing parameter X_t with the (known) value of the Higgs mass M_h. In other words, for each set of $\tan\beta$ and M_A inputs, one selects the ϵ radiative correction that leads to the correct mass $M_h = 126$ GeV. The LHC constraint on the mass of the observed Higgs state is then automatically satisfied. We emphasize again that for the large SUSY scales that are needed for the low $\tan\beta$ regime, $\tan\beta \lesssim 3$, the MSSM spectrum cannot be calculated in a reliable way using the usual versions of the RGE programs such as `Suspect`.

A second constraint comes from the measurement of the production and decay rates of the observed Higgs particle. The ATLAS and CMS collaborations have provided the signal strength modifiers μ_{XX}, that are identified with the Higgs cross section times decay branching ratio normalized to the SM expectation in a given $H \to XX$ search channel. For the various search channels that have been conducted, $h \to ZZ, WW, \gamma\gamma, \tau\tau$ and $b\bar{b}$ with the entire set of data collected in the runs at $\sqrt{s} = 7$ TeV and 8 TeV, i.e. ≈ 5 fb^{-1} and ≈ 20 fb^{-1} (with the exception of $h \to b\bar{b}$ which has been analyzed only with 17 fb^{-1} of the 7+8 TeV data) numbers can be found in Refs. [66–75]. These should be used to constrain the couplings of the h state and, hence, the $[\tan\beta, M_A]$ parameter space.

Rather than performing a complete fit of the ATLAS and CMS light Higgs data including all the signal strengths, we will simply use the most precise and cleanest observable in this context: the signal strength μ_{ZZ} in the search channel $h \to ZZ$. As recently discussed in Ref. [78] (to which we refer for the details), this channel is fully inclusive and does not

involve the additional large theoretical uncertainties that occur when breaking the cross section of the dominant production process $gg \to h$ into jet categories[9]. In addition, contrary to the global signal strength $\mu_{\rm tot}$, it does not involve the channel $h \to \gamma\gamma$ which, at least in the ATLAS case, deviates from the SM prediction and might indicate the presence of new contributions (such as those of light charginos?) in the $h\gamma\gamma$ loop. The combination of the ATLAS and CMS data in the ZZ channel gives, $\mu_{ZZ} = 1,10 \pm 0.22 \pm 0.20$ where the first uncertainty is experimental and the second one theoretical. Following Ref. [42], we assume a total theoretical uncertainty of $\Delta^{\rm th} = \pm 20\%$ and, since it should be considered as a bias, we add it linearly to the experimental error. This gives a lower limit on the $h \to ZZ$ signal strength of $\mu_{ZZ} \gtrsim 0.62$ at 68%CL and $\mu_{ZZ} \gtrsim 0.4$ at 95%CL.

In the MSSM case, the signal strength will be given by $\mu_{ZZ} = \sigma(h) \times {\rm BR}(h \to ZZ)/\sigma(H_{\rm SM}) \times {\rm BR}(H_{\rm SM} \to ZZ)$ and will be thus proportional to combinations of reduced h coupling squared to fermions and gauge bosons, $g^2_{htt} \times g^2_{hVV}/g^2_{hbb}$... The fact that μ_{ZZ} can be as low at 0.4 at 95%CL means that we can be substantially far from the decoupling limit, $g^2_{HVV} \approx 0.1$, with not too heavy $H/A/H^\pm$ states even at low $\tan\beta$.

In Fig. 6, we have scanned the $[\tan\beta, M_A]$ parameter space and delineated the areas in which the 68%CL and 95%CL constraints on μ_{ZZ} are fulfilled. We observe that indeed, the entire range with $M_A \lesssim 200$ GeV for most value of $\tan\beta$ is excluded at the 95%CL. With increasing $\tan\beta$, the excluded M_A values are lower and one recovers the well known fact that the decoupling limit is reached more quickly at higher $\tan\beta$ values. In most cases, we will use this indirect limit of $M_A \lesssim 200$ GeV prior to any other constraint (except for illustrations in the $H^\pm$ case where the low mass range will be kept).

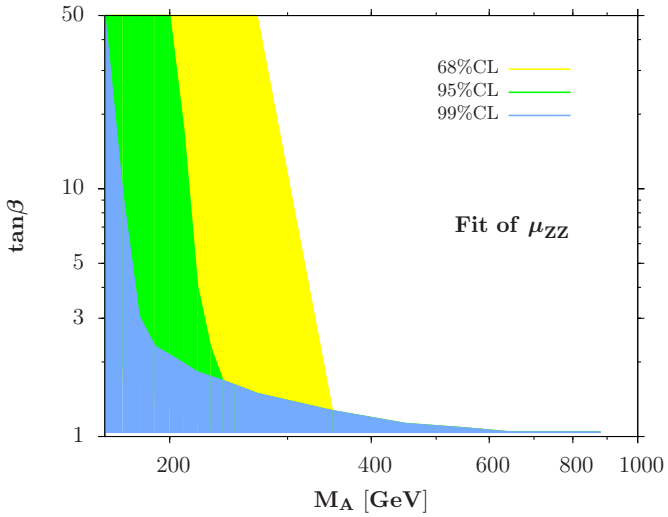

Figure 6: The $[\tan\beta, M_A]$ parameter space of the MSSM in which the signal strength in the $h \to ZZ$ search channel is compatible with the LHC data on the rates of the observed h boson at the 68%CL (green), 95%CL (yellow) and 99%CL (blue).

[9]For instance, the signal strengths is the $\tau\tau$ and WW channels are obtained by considering the $gg \to H + 0j, 1j$ and/or the vector boson fusion categories. The signal strength μ_{WW} provides the same information as μ_{ZZ}, while the measurement of the signal strengths in the $h \to b\bar{b}$ and $h \to \tau^+\tau^-$ channels are not yet very accurate. Hence, using only the $h \to ZZ$ channel should be a good approximation.

4.2 Constraints from the heavier Higgs searches at high $\tan\beta$

As discussed in section 3.1, the most efficient channel to search for the heavier MSSM Higgs bosons is by far H/A production in gg and $b\bar{b}$ fusion with the Higgs bosons decaying into τ lepton pairs, $pp \to \Phi \to \tau^+\tau^-$. Searches for this process have been performed by the ATLAS collaboration with ≈ 5 fb^{-1} data at the 7 TeV run [74] and by the CMS collaboration with $\approx 5 + 12$ fb^{-1} data at the 7 TeV and 8 TeV runs [75]. Upper limits on the production times decay rates of these processes (which, unfortunately, have not given by the collaborations) have been set and they can be turned into constraints on the MSSM parameter space which, in the Higgs sector, corresponds to the $[\tan\beta, M_A]$ plane.

In Fig. 7, we display the sensitivity of the CMS $\Phi \to \tau\tau$ analysis in the $[\tan\beta, M_A]$ plane. The excluded region, obtained from the observed limit at the 95%CL is drawn in light blue. The solid line represents the median expected limit which turns out to be weaker than the observed limit. As can be seen, this constraint is extremely restrictive and for values $M_A \lesssim 250$ GeV, it excludes almost the entire intermediate and high $\tan\beta$ regimes, $\tan\beta \gtrsim 5$. The constraint is of course less effective for a heavier pseudoscalar Higgs boson, but even for $M_A = 400$ GeV the high $\tan\beta \gtrsim 10$ region is excluded and one is even sensitive to large values $M_A \approx 700$ GeV for $\tan\beta \gtrsim 50$.

There are, however, some caveats to this exclusion limit as discussed in section 3.1. The first one is that there is a theoretical uncertainty that affects the Higgs production cross section times decay branching ratios which is of the order of $\pm 25\%$ when the $gg \to \Phi$ and $b\bar{b} \to \Phi$ cross sections are combined. If this theoretical uncertainty is included when setting the limit in the $[\tan\beta, M_A]$ plane, as shown by the dashed contours around the expected limit in Fig. 7, the constraint will be slightly weaker as one then needs to consider the lower value of the $\sigma(pp \to \Phi) \times \text{BR}(\Phi \to \tau^+\tau^-)$ rate predicted by theory.

The second caveat is that the CMS (and ATLAS) constraint has been given in a specific benchmark scenario, the maximal mixing scenario with the choice $X_t/M_S = \sqrt{6}$ and the value of the SUSY scale set to $M_S = 1$ TeV; the other parameters such as the gaugino and higgsino masses and the first/second generation fermion parameters that have little impact can be chosen as in eq. (2.7). However, as was previously argued, the $pp \to \Phi \to \tau\tau$ cross section times decay branching fraction is very robust and, hence, the exclusion limit is almost model independent. It is altered only very mildly by the radiative corrections in the MSSM Higgs sector, in particular by the choice of the parameters M_S and X_t (this is especially true if these parameters are to be traded against the measured values of M_h).

In fact, the exclusion limit in Fig. 7 can be obtained in any MSSM scenario with the only assumption being that SUSY particles are too heavy to affect $\sigma(pp \to \Phi) \times \text{BR}(\Phi\tau\tau)$ by more than 25%, which is the estimated theoretical uncertainty. Even in the case of light SUSY particles, it is very hard to make that stop/sbottom squarks contribute significantly to the $gg \to H$ production processes, or to have a significant Δ_b correction to the Φbb coupling which largely cancels out as indicated by eq. (2.12), or to have a substantial change of the $\Phi \to \tau\tau$ fraction due to light SUSY particles that appear in the decays.

Thus, the limit for the $pp \to \tau^+\tau^-$ searches is robust with respect to the SUSY parameters and is valid in far more situations and scenarios than the "MSSM M_h^{max} scenario"

that is usually quoted by the experimental collaborations. We thus suggest to remove this assumption on the benchmark scenario (in particular it adopts the choice $M_S = 1$ TeV which does not allow low $\tan\beta$ values and which starts to be challenged by direct SUSY searches), as the only relevant assumption, if any, should be that we do not consider cases in which the SUSY particles are too light to alter the Higgs production and decay rates. This is a very reasonable attitude if we are interested mainly in the Higgs sector.

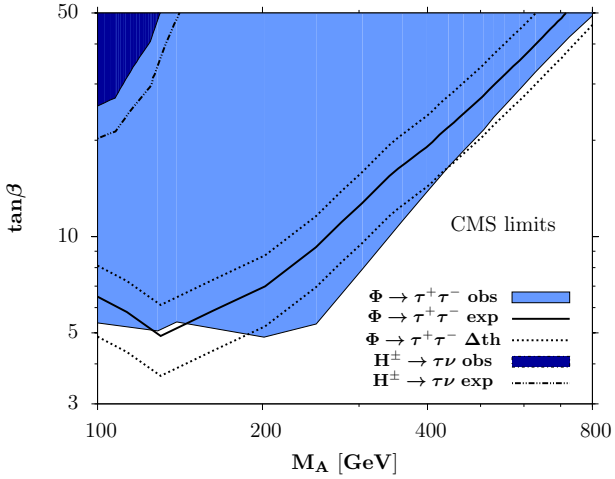

Figure 7: The $[\tan\beta, MA]$ plane in the MSSM in which the $pp \to H/A \to \tau^+\tau^-$ (light blue) and $t \to bH^+ \to b\tau\nu$ (dark blue) search constraints using the CMS data are included (observed limits). The solid contour for the $pp \to \tau\tau$ mode is for the median expected limit and the two dashed ones are when the QCD uncertainties on the rates are included.

Another constraint on the MSSM Higgs sector[10] is the one from charged Higgs searches in the $H^- \to \tau\nu$ final states with the $H^\pm$ bosons produced in top quark decays, $t \to H^+b \to \tau\nu b$. Up to now, the ATLAS and CMS collaborations have released results only with the ≈ 5 fb^{-1} collected at $\sqrt{s} = 7$ TeV [76, 77]. We have also delineated in Fig. 7 the impact on the $[\tan\beta, MA]$ parameter space of the CMS 95%CL observed limits in this channel.

As can be observed, the constraint is effective only for values $M_A \lesssim 150$ GeV which correspond to a light H^+ state that could be produced in top quark decays. The search is sensitive to the very high $\tan\beta$ region which is completely excluded by the $\tau\tau$ search, that is performed with much more data though. However, even if the comparison is made for the same amount of data, he $pp \to \Phi \to \tau\tau$ search is by far more sensitive.

Note that contrary to the $pp \to \tau^+\tau^-$ case, the limits at high $\tan\beta$ from the process $pp \to t\bar{t}$ with $t \to bH^+ \to b\tau\nu$ might be more model dependent. Indeed, while SUSY decays might not be important as the small $M_{H^\pm}$ value leaves little room for light sparticles (and the high $\tan\beta$ values would suppress these decays anyway), the effect of the Δ_b corrections might be larger as there is no cancellation between production and decay rates. Nevertheless, the $H^\pm$ limit is effective only for $M_A \lesssim 150$ GeV values excluded by the h data. We keep this $H^\pm$ constraint though, as it is also valid in two-Higgs doublet models.

[10] A search has also been performed by the CMS collaboration based on the 7 TeV data in the channel $pp \to \Phi b\bar{b} \to bbbb$ [57]. This search is much less sensitive than the $\tau\tau$ search even if one extrapolates the expected limits to the same amount of data. We will thus ignore it in our study.

4.3 Extrapolation to the low $\tan\beta$ region and the full 7+8 data

A very important remark is that in our version of the constraints in the $[\tan\beta, M_A]$ plane of Fig. 7, we have removed the region excluded by the bound on the h mass, $M_h \gtrsim 114$ GeV from negative Higgs searches at LEP2, which is also usually displayed by the experimental collaborations. In the usual benchmark scenario, this constraint excludes the entire low $\tan\beta$ regime, $\tan\beta \lesssim 3$, and at low $M_A \approx 100$ GeV, $\tan\beta$ values up to $\tan\beta \approx 10$.

A first reason for removing the "LEP exclusion" region is that it is now superseded by the "observation" constraint 123 GeV $\lesssim M_h \lesssim$ 129 GeV (once the theoretical and experimental uncertainties are included) which is by far stronger. In fact, as was discussed in Ref. [29], if the benchmark scenario with $M_S = 1$ TeV and maximal stop mixing is to be adopted, the entire range $\tan\beta \lesssim 5$ and $\tan\beta \gtrsim 20$ for any M_A value would be excluded simply by requiring that 123 GeV $\lesssim M_h \lesssim$ 129 GeV (and the excluded regions would be completely different for other M_S and X_t values as also shown in Ref. [29]).

A second reason is that the LEP2 M_h constraint and even the constraint $M_h \gtrsim 123$ GeV can be simply evaded for any value of $\tan\beta$ or M_A by assuming large enough M_S values as discussed in section 2.1. This will then open the very interesting low $\tan\beta$ region which can be probed in a a model independent way by Higgs search channels involving the $H, A, H^\pm$ bosons, including the $t \to bH^+ \to b\tau\nu$ channel discussed previously.

Indeed, the branching fraction for the decay $t \to bH^+$ is also significant at low $\tan\beta$ values, when the component of the coupling g_{tbH^+} that is proportional to $\bar{m}_t/\tan\beta$ becomes dominant. On the other hand, the branching fraction for the decay $H^\pm \to \tau\nu$ stays close to 100%. Hence, the rates for $pp \to t\bar{t}$ with $t \to bH^+ \to b\tau\nu$ are comparable for $\tan\beta \approx 3$ and $\tan\beta \approx 30$ and the processes can also probe the low $\tan\beta$ region. This is exemplified in Fig. 8 where the $t \to bH^+$ CMS median expected and observed limits obtained with the 7 TeV data are extrapolated to the low $\tan\beta$ region. As can be seen, the region $\tan\beta \lesssim 2$ is excluded for $M_A \lesssim 140$ GeV (this region can also be probed in the $H^+ \to c\bar{s}$ mode).

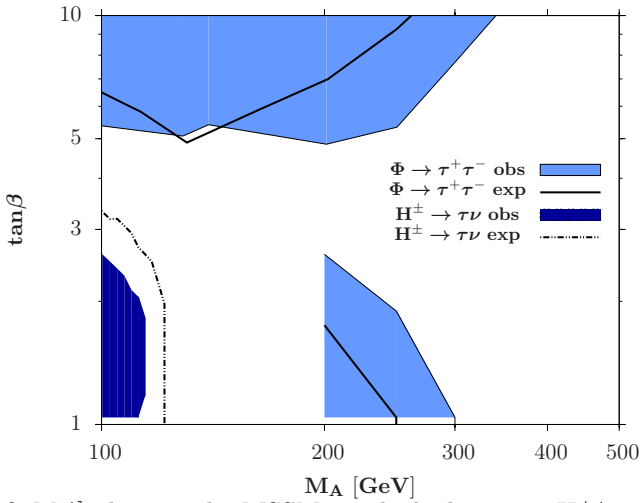

Figure 8: The $[\tan\beta, MA]$ plane in the MSSM in which the $pp \to H/A \to \tau^+\tau^-$ (light blue) and $t \to bH^+ \to b\tau\nu$ (dark blue) observed limits using the CMS data are extrapolated to low $\tan\beta$. The solid contours in the $\tau\tau$ and $\tau\nu$ cases are for the expected limits.

In fact, as is shown in the lower part of Fig. 8, even the channel $pp \to \Phi \to \tau\tau$ is useful

at low $\tan\beta$. Indeed, for $\tan\beta$ values close to unity, while the $b\bar{b} \to \Phi$ process becomes irrelevant, the cross sections for the $gg \to \Phi$ process becomes very large, the reason being that for $\tan\beta \approx 1$ the couplings $g_{\Phi tt} \propto \bar{m}_t/\tan\beta$ are significant and the dominant top quark loop contribution becomes less suppressed compared to the SM. On the other hand, at least in the case of the pseudoscalar A, the branching ratio for the $\tau^+\tau^-$ decay stays significant for M_A values up to the $t\bar{t}$ threshold as shown in Fig. 4. Hence, the production times decay rate for $gg \to A \to \tau\tau$ stays large and the CMS search limit is effective and excludes $\tan\beta$ values close to 1, for pseudoscalar masses up to $M_A \approx 350$ GeV.

One would get a better feeling of the power of these constraints at low $\tan\beta$ values (and in the charged Higgs case also at high $\tan\beta$), if the present limits in the $pp \to \tau\tau$ and $t \to bH^+ \to b\tau\nu$ channels are extrapolated to the full set of data collected in the 2011 and 2012 LHC runs. This is shown in Fig. 9 where the median expected CMS limits in the two search channels are extrapolated to an integrated luminosity of 25 fb^{-1}, assuming that the limits simply scale like the square–root of the number of events.

The gain in sensitivity is very significant in the $H^\pm$ case as the gap between the present CMS limit with the ≈ 5 fb^{-1} of the 7 TeV data and the expected limit with the additional ≈ 20 fb^{-1} data at 8 TeV is large (there is an additional increase of the $pp \to t\bar{t}$ production cross section from $\sqrt{s} = 7$ TeV to 8 TeV). In the case of the $pp \to \tau\tau$ channel, the increase of sensitivity is much more modest, not only because the gap from the 17 fb^{-1} data used in the latest CMS analysis and the full 25 fb^{-1} data collected up to now is not large but, also, because presently the observed limit is much stronger than the expected limit.

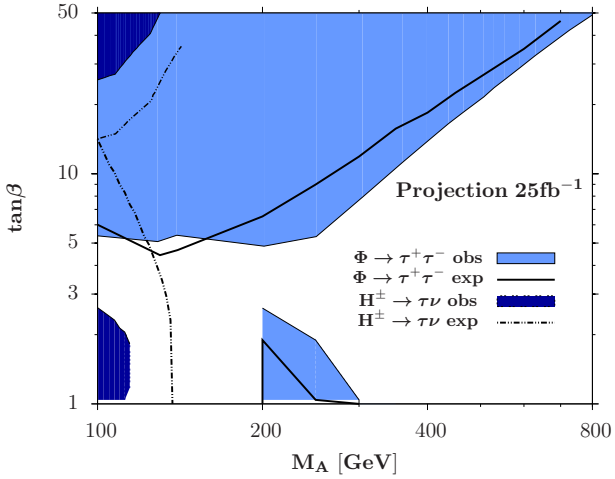

Figure 9: The $[\tan\beta, MA]$ plane in the MSSM in which the $pp \to H/A \to \tau^+\tau^-$ and $t \to bH^+ \to b\tau\nu$ CMS expected limits are extrapolated to the full 7+8 TeV data with ≈ 25 fb^{-1}. The present observed limits are still shown in blue.

Hence, these interesting low $\tan\beta$ areas that were thought to be buried under the LEP2 exclusion bound on M_h are now open territory for heavy MSSM Higgs hunting. This can be done not only in the two channels $pp \to \tau^+\tau^-$ and $t \to bH^+ \to b\tau\nu$ above (and which were anyway used at high $\tan\beta$) but also in a plethora of channels that have not been discussed before (or at least abandoned after the LEP2 results) and to which we turn now.

5. Heavy Higgs searches channels at low $\tan\beta$

We come now to the main phenomenological issue of this paper: the probe at the LHC of the low $\tan\beta$ region for a not too heavy pseudoscalar A state[11]. We stress again that this region can be resurrected simply by allowing a large SUSY scale M_S which removes the LEP2 $M_h \gtrsim 114$ GeV constraint (and now the LHC mass constraint $M_h \approx 126$ GeV). We show that several channels discussed in the case of a high mass SM Higgs or in scenarios beyond the SM can be used for the search of the MSSM H, A and $H^\pm$ bosons.

5.1 The main search channels for the neutral H/A states

5.1.1 The H $\to$ WW, ZZ channels

These are possible only for the heavier H boson (because of CP invariance there are no VV couplings for A) with masses below the $t\bar{t}$ threshold where the branching ratios for the decays $H \to WW$ and $H \to ZZ$ are significant; see Fig. 4. The $H \to WW$ process is particularly useful in the region $160 \lesssim M_H \lesssim 180$ GeV where the branching ratio is close to 100%. In both cases, the $gg \to H$ production process can be used but, eventually, vector boson fusion can also be relevant at the lowest $\tan\beta$ and M_H possible values.

The search modes that are most useful at relatively low M_H values, should be the $pp \to H \to ZZ \to 4\ell^\pm$ and $pp \to H \to WW \to 2\ell 2\nu$ channels that have been used to observe the SM–like light h boson (as the mass resolution of the $H \to WW$ channel is rather poor, one has to subtract the observed signal events in the low mass range, $M_H \lesssim 160$ GeV) and to exclude a SM–like Higgs particle with a mass up to 800 GeV [69, 71]. When the two processes are combined, the sensitivity is an order of magnitude larger than for the SM Higgs for masses below 400 GeV and one can thus afford a substantial reduction of the couplings g_{Htt} and g_{HVV} which should allow to probe $\tan\beta$ values significantly higher than unity[12]. At high H masses, $M_H \gtrsim 300$ GeV, one could also add the $pp \to H \to ZZ \to 2\ell 2q, 2\nu 2q, 2\ell 2\nu$ and $pp \to H \to WW \to \ell\nu 2q$ channels to increase the statistics, as done in a recent study by the CMS collaboration [81].

There is one difference with the SM Higgs case though. While in the SM, the Higgs particle has a large total width at high masses as a result of the decays into longitudinal W/Z bosons which make it grow as $M^3_{H_{\rm SM}}$, the MSSM H boson remain narrow as the coupling g_{HVV} is suppressed. In fact, all MSSM Higgs particles will have a total width that is smaller than ≈ 3 GeV for $\tan\beta \approx 3$ and masses below 500 GeV. The smaller total width in the MSSM can be rather helpful at relatively high H masses as, for instance, it allows to suppress the continuum ZZ background by selecting smaller bins for the invariant

[11] This issue has been discussed in the past and a summary can be found in section 3.3.2 of Ref. [7]. It has been also addressed recently in Ref. [53] (where, in particular, a feasibility study of the $H \to hh$ and $A \to hZ$ modes at $\sqrt{s} = 14$ TeV is made) and in talks given the last months by one of the authors [79]. Recent analyses of heavier MSSM Higgsses at intermediate and high $\tan\beta$ can be found in Ref. [80].

[12] The ATLAS collaboration has recently analyzed heavy H production in a two–Higgs doublet model in the channel $H \to WW \to e\nu\mu\nu$ with 13 fb^{-1} data collected at $\sqrt{s} = 8$ TeV [82]. Unfortunately, this analysis cannot readily be used as the limit on the cross section times branching fraction has not been explicitly given and the results are displayed in terms of $\cos(\alpha)$ (and not $\cos(\beta - \alpha)$ which would have corresponded to the HWW coupling) which does not allow an easy interpretation in the MSSM.

mass of the ZZ system in the signal events. Issues like the interference of the signal and the $gg \to VV$ backgrounds will also be less important than in the SM.

5.1.2 The H/A $\to t\bar{t}$ channels

This search channel has not been considered in the case of the SM Higgs boson for two reasons [4]. The first one is that for $M_{H_{\rm SM}} \gtrsim 350$ GeV, the $H_{\rm SM} \to WW, ZZ$ channels are still relevant and largely dominate over the $H_{\rm SM} \to t\bar{t}$ decay channel which has a branching fraction that is less than 20% in the entire Higgs mass range (the reason being again that the partial widths for $H_{\rm SM} \to VV$ grow as $M^3_{H_{\rm SM}}$ while for $H_{\rm SM} \to t\bar{t}$ its grows only like $M_{H_{\rm SM}}$). The other reason is that the continuum $t\bar{t}$ background was thought to be overwhelmingly large as it had to be evaluated in a large mass window because of the large Higgs total width (in addition, the events from $H_{\rm SM} \to t\bar{t}$ produce a dip–peak structure in the $gg \to t\bar{t}$ invariant mass spectrum that was unobservable for a large total width).

The situation in the MSSM is very different. First, as mentioned previously, the total width for heavy H and A states are much smaller, less than $\lesssim 20$ GeV for any $\tan\beta \gtrsim 1$ value for $M_{H,A} \lesssim 500$ GeV and grow (almost) linearly with the Higgs masses beyond this value. One can thus integrate the $t\bar{t}$ continuum background in a smaller invariant mass bin and significantly enhance the signal to background ratio. A second feature is that contrary to the SM case, the branching ratios for the $H/A \to t\bar{t}$ decays are almost 100% for $\tan\beta \lesssim 3$ as soon as the channels are kinematically open (this is particularly true for A where even below the threshold, the three–body decay $A \to tt^* \to tbW$ is important).

The only disadvantage compared to the SM is that the production cross section could be smaller. In the MSSM, the only relevant process in the low $\tan\beta$ regime for $M_\Phi \gtrsim 350$ GeV is $gg \to \Phi$ with the dominant (almost only) contribution being due to the top quark loop. The latter is suppressed by the square of the coupling $g_{\Phi tt} \propto 1/\tan\beta$ if $\tan\beta$ is not close to unity. However, in the MSSM, one has to add the cross sections of both the H and A states. In addition, the loop form factors in the pseudoscalar A and scalar $H/H_{\rm SM}$ cases are different and, as can been seen from Fig. 3, the $gg \to \Phi$ cross section is larger in the pseudoscalar Higgs case when the same top Yukawa coupling is assumed.

In toto, the situation for $H/A \to t\bar{t}$ will certainly be more favorable for the MSSM at low $\tan\beta$ than in the SM. While there was no search for the SM Higgs in this channel, the ATLAS [83] and CMS [84] collaborations have looked for heavy resonances (such as new Z' gauge bosons in extended gauge models or Kaluza–Klein excitations in scenarios with extra space–time dimensions) that decay into $t\bar{t}$ pairs with the data collected at the 7 TeV run. The lepton+jets final state has been studied in the topology where the top quarks are highly boosted which allows a good discrimination from the continuum $t\bar{t}$ background [85] (the ATLAS and CMS collaborations searches assume resonance masses $M_{tt} \gtrsim 700$ GeV to benefit from this topology). Limits on the cross sections times branching ratios have been set, corresponding to roughly $\sigma_{tt} \approx 0.7$ pb for a resonance with a mass of 1 TeV and a narrow width, $\Gamma_{tt} \approx 10^{-2} M_{tt}$ (which is more or less the case of the MSSM H/A states at $\tan\beta \approx 3$). A lower (higher) cross section is needed at larger (smaller) resonance mass when the top quarks are (not) sufficiently boosted and, at $M_{tt} \approx 500$ GeV, one needs $\sigma_{tt} \approx 3$ pb which approximately corresponds to an increase with $1/M^2_{tt}$.

5.1.3 The A → Zh channel

As discussed earlier, the $gg \to A$ production cross section is very large at low $\tan\beta$ values: it is higher than for the SM Higgs boson at $\tan\beta = 1$ (as the form factor for the ggA amplitude is larger than in the scalar Higgs case) and is suppressed only by a factor $g^2_{Att} \propto 1/\tan^2\beta$. On the other hand, in the range $M_h + M_Z \lesssim M_A \lesssim 2m_t$, the branching ratio for the decay $A \to hZ$ is large for $\tan\beta \approx 3$ and largely dominant for $\tan\beta \approx 1$. In the mass window $M_A = 210$–350 GeV, the production times decay rate for the process $gg \to A \to hZ$ should be thus very high in the low $\tan\beta$ region.

The hZ final state has been searched for in the SM in the Higgs–strahlung process, $q\bar{q} \to Z^* \to Zh$ with the Z boson decaying into leptons or neutrinos, $Z \to \ell^+\ell^-, \nu\bar{\nu}$ and the h boson decaying into $b\bar{b}$ final states [72, 73]. The significance of the signal is strongly increased by looking at boosted jets when the Higgs has a large transverse momentum [86]. In the CMS analysis with 17 fb^{-1} of the 2011 and 2012 data [73], a signal strength $\mu_{bb} \approx 1.5$ has been found in the $Z \to \nu\bar{\nu}$ and $Z \to \ell^+\ell^-$ channels with a large error bar. Very roughly, one can assume that the additional events from the $A \to Zh$ channel should be observed if they exceed this sensitivity when extrapolated to include the full 2012 data.

One should note that the information from the $pp \to Zh$ search in the SM provides only a lower limit for the sensitivity as in the present case one can benefit from the fact that the invariant mass of the four fermion final state (without neutrinos) which should peak at the value M_A will further suppress the continuum background, in particular the $Z + b\bar{b}$ events. However, as h is originating from the decay of the state A which should not be very heavy, it has not enough transverse momentum to strengthen the boosted jet techniques that allow to isolate the $h \to b\bar{b}$ signal from the QCD background.

5.1.4 The H → hh channel

The channel $pp \to H \to hh$ is similar to $A \to hZ$: it has very large production rates in the low $\tan\beta$ regime in the mass range 250 GeV $\lesssim M_H \lesssim$ 350 GeV when the decay channels $H \to hh$ is kinematically open and the $H \to t\bar{t}$ mode is closed; the $gg \to H$ cross section should be substantial in this area of the parameter space.

If the dominant $h \to b\bar{b}$ decay is considered, the signal topology has some similarities with that of the process $gg \to b\bar{b} + A/H$ which was discussed here as being one of the main MSSM Higgs processes at high $\tan\beta$ and searched for by the CMS collaboration with the 7 TeV data [57]. However, the kinematical behavior is very different and in the signal events, one can use further constraints, $M_{bb} \approx M_h$ and $M_{bbbb} \approx M_H$ (see Ref. [53] where a characterization of this channel has been made). In fact, the $H \to hh$ channel has more similarities with double production of the SM–like Higgs boson, $gg \to hh$, which is considered for the measurement of the Higgs self–coupling a the 14 TeV LHC with a high luminosity. This process has been revisited recently [87] and it has been shown that the final state channels $b\bar{b}\tau\tau$ and $b\bar{b}\gamma\gamma$ would be viable at $\sqrt{s} = 14$ TeV and $\mathcal{L} \gtrsim 300$ fb^{-1}. Because the $h \to \gamma\gamma$ decay is too rare, only the first process could be considered at $\sqrt{s} = 8$ TeV with 25 fb^{-1} data. Note that here again, one could use the reconstructed H mass constraint, $M_H = M_{hh}$, to further suppress the continuum background.

5.2 Expectations for the LHC with 25 fb^{-1} data

It is obvious that a truly reliable estimate of the sensitivity on the heavy neutral MSSM Higgs bosons in the various channels discussed before can only come from the ATLAS and CMS collaborations. We will nevertheless attempt in this section to provide a very rough estimate of the achievable sensitivities using present searches conducted for a heavy SM Higgs and in beyond the SM scenarios. The very interesting results that could be obtained would hopefully convince the experimental collaborations to conduct analyses in this area.

Following the previous discussions, our working assumptions to derive the possible sensitivities in the various considered search channels are as follows:

– $H \to WW, ZZ$: we will use the recently published CMS analysis of Ref. [81] that has been performed with the ≈ 10 fb^{-1} data collected in the 7+8 TeV runs and in which all possible channels $H \to ZZ \to 4\ell, 2\ell 2\nu, 2\ell jj, 2\nu jj$ and $H \to WW \to 2\ell 2\nu, \ell\nu jj$ have been included and combined. In the entire range $M_H = 160$–350 GeV, where the SM Higgs boson almost exclusively decays into WW or ZZ states, we will assume the cross section times decay branching ratio upper limit that has been given in this CMS study,

– $H/A \to t\bar{t}$: we make use of the ATLAS [83] and CMS [84] searches at $\sqrt{s} = 7$ TeV for new Z' or Kaluza–Klein gauge bosons that decay into $t\bar{t}$ pairs in the lepton+jets final state topology. Considering a small total width for the resonance, limits on the cross sections times branching ratio of $\approx 6, 3$ and 0.75 pb for a resonance mass of, respectively, 350, 500 and 1000 GeV are assumed. This is equivalent to a sensitivity that varies with $1/M_{tt}^2$ that we will optimistically assume to also cover the low mass resonance range.

– $A \to hZ$: we will use the sensitivity given by ATLAS [72] and CMS [73] in their search for the SM Higgs–like strahlung process $pp \to hZ$ with $h \to b\bar{b}$ and $Z \to \ell\ell, \nu\bar{\nu}$, $\sigma/\sigma^{\rm SM} = 2.8$ with 17 fb^{-1} data at $\sqrt{s} = 7 + 8$ TeV (we have included the error bar). This should be sufficient as, in addition, we would have on top the constraint from the reconstructed mass in the $\ell\ell b\bar{b}$ channel which is not used in our analysis.

– $H \to hh$: we use the analysis of the process $gg \to hh$ in the SM performed in Ref. [87] for the 14 TeV LHC that we also scale down to the current energy and luminosity. The final state $bb\tau\tau$ final state will be considered, with the assumption that the cross section times branching ratio should be larger than $\sigma \times {\rm BR} \sim 500$ fb for illustration.

The results are shown in Fig. 10 with an extrapolation to the full 25 fb^{-1} data of the 7+8 TeV LHC run. Again, we assumed that the sensitivity scales simply as the square root of the number of events. The sensitivities from the usual $H/A \to \tau^+\tau^-$ and $t \to bH^+ \to b\tau\nu$ channels are also shown. The green and red areas correspond to the domains where the $H \to VV$ and $H/A \to t\bar{t}$ channels become constraining with the assumptions above. The sensitivities in the $H \to hh$ and $A \to hZ$ modes are given by, respectively, the yellow and brown areas that peak in the mass range $MA = 250$–350 GeV visible at very low $\tan\beta$ values. We refrain from extrapolating to the LHC with 14 TeV c.m. energy.

The outcome is impressive. These channels, in particular the $H \to VV$ and $H/A \to t\bar{t}$ processes, are very constraining as they cover the entire low $\tan\beta$ area that was previously excluded by the LEP2 bound up to $M_A \approx 500$ GeV. Even $A \to hZ$ and $H \to hh$ are visible in small portions of the parameter space at the upgraded LHC.

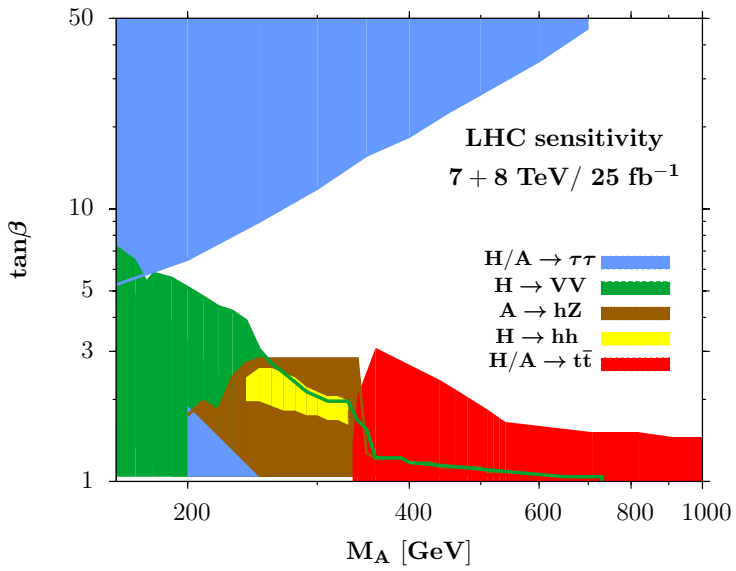

Figure 10: The estimated sensitivities in the various search channels for the heavier MSSM Higgs bosons in the $[\tan\beta, M_A]$ plane: $H/A \to \tau^+\tau^-$ (light blue), $t \to H^+b \to \tau\nu b$ (dark blue), $H \to WW + ZZ$ (green), $H/A \to t\bar{t}$ (red), $A \to hZ$ (brown) and $H \to hh$ (yellow). The projection is made for the LHC with 7+8 TeV and the full 25 fb^{-1} of data collected so far. The radiative corrections are such that the lightest h mass is $M_h = 126$ GeV.

5.3 Remarks on the charged Higgs boson

We close this discussions with a few remarks on the charged Higgs boson case. First of all, the production rates are very large only for $M_{H^\pm} \lesssim 170$ GeV when the $H^\pm$ state can be produced in top decays. In this case, the decay channel $H^\pm \to \tau\nu$ is always substantial and leads to the constraints that have been discussed earlier and which are less effective than those coming from $H/A \to \tau\tau$ searches at high $\tan\beta$. In the low $\tan\beta$ region, two other channels can be considered: $H^+ \to c\bar{s}$ that has been studied by the ATLAS collaboration in a two–Higgs doublet model with the 7 TeV data [88] and $H^+ \to c\bar{b}$. The branching ratio for the latter channel is significant for $\tan\beta \lesssim 3$ and has been obtained by assuming the same CKM angles as in the SM, in particular $V_{cb} \approx 0.04$ [34]. This channel, if observed would thus allow to check some of the CKM matrix elements in the charged Higgs sector.

Finally, the processes $t \to H^+b$ at low mass and $pp \to btH^\pm$ at high mass with $H^\pm \to Wh$ can have large rates at sufficiently low $\tan\beta$. The cross section times branching fraction is displayed in Fig. 11 in the $[\tan\beta, M_A]$ plane for a 14 TeV c.m. energy. Shown are the contours with $\sigma \times \text{BR} = 1.10$ and 30 fb which, for a luminosity of 300 fb^{-1} would correspond to a small number of events. We will not perform an analysis for this particular final state. We simply note that the final state topology, $pp \to tbH^\pm \to tbWh$ resembles that of the $pp \to t\bar{t}h$ process that is considered as a means to measure the $ht\bar{t}$ Yukawa coupling and which is considered to be viable at 14 TeV with a high luminosity.

Hence, even for the charged Higgs bosons, there are interesting search channels which can be considered if the low $\tan\beta$ region is reopened.

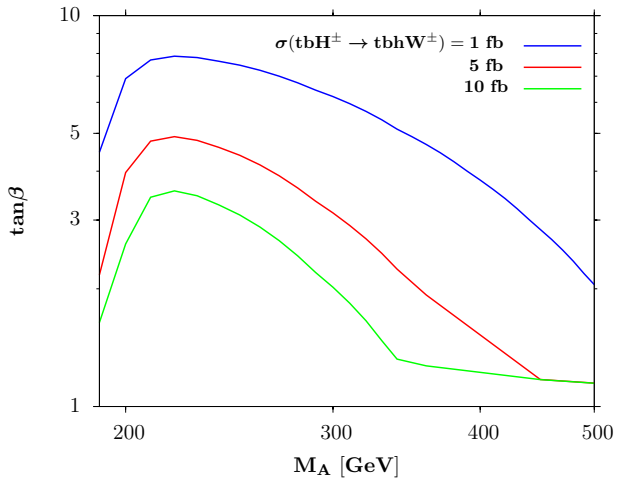

Figure 11: The production cross sections times decay branching ratio at the LHC with $\sqrt{s} = 14$ TeV for the process $pp \to t\bar{b}H^- + \bar{t}bH^+$ with $H^\pm \to hW^\pm$ in the $[\tan\beta, M_A]$ plane. The contours are for some (rough estimates of) limiting values of $\sigma \times$ BR.

6. Conclusions

After the observation of the 126 GeV SM–like Higgs boson by the ATLAS and CMS collaborations, the next challenge at the LHC should be to search for new phenomena beyond the SM. This can be done not only by refining the precision determination of the properties of the observed Higgs particle to pin down small deviations of its couplings from the SM expectations, but also by looking for the direct production of new states.

In this paper, we have considered the production of the heavier H, A and $H^\pm$ bosons of the MSSM at the LHC, focusing on the low $\tan\beta$ regime, $\tan\beta \lesssim 3$–5. We have first shown that this area of the MSSM parameter space, which was long thought to be excluded, is still viable provided that the SUSY scale is assumed to be very high, $M_S \gtrsim 10$ TeV. For such M_S values, the usual tools that allow to determine the masses and couplings of the Higgs and SUSY particles in the MSSM, including the higher order corrections, become inadequate. We have used a simple but not too inaccurate approximation to describe the radiative corrections to the Higgs sector, in which the unknown scale M_S and stop mixing parameter X_t are traded against the measured h boson mass, $M_h \approx 126$ GeV. One would then have, to a good approximation, only two basic input parameters in the MSSM Higgs sector even at higher orders: $\tan\beta$ and M_A, which can take small values, $\tan\beta \approx 1$ and $M_A = \mathcal{O}(200)$ GeV, provided that M_S is chosen to be sufficiently large.

In the low $\tan\beta$ region, there is a plethora of new search channels for the heavy MSSM Higgs bosons that can be analyzed at the LHC. The neutral H/A states can be still be produced in the gluon fusion mechanism with large rates, and they will decay into a variety of interesting final states such as $H \to WW, ZZ$, $H \to hh$, $H/A \to t\bar{t}$, $A \to hZ$. Interesting decays can also occur in the case of the charged Higgs bosons, e.g. $H^+ \to hW, c\bar{s}, c\bar{b}$. These modes come in addition to the two channels $H/A \to \tau^+\tau^-$ and $t \to bH^+ \to b\tau\nu$ which are currently being studied by ATLAS and CMS and which are very powerful in constraining the parameter space at high $\tan\beta$ values and, as is shown here, also at low $\tan\beta$ values.

We have shown that already with the current LHC data at $\sqrt{s} = 7$+8 TeV, the area with small $\tan\beta$ and M_A values can be probed by simply extrapolating to the MSSM Higgs sector the available analyses in the search of the SM Higgs boson at high masses in the WW and ZZ channels and the limits obtained in the $t\bar{t}$ channels in the search for high–mass new gauge bosons from extended gauge or extra–dimensional theories. The sensitivity in these channels will be significantly enhanced at the 14 TeV LHC run once 300 fb^{-1} data will be collected. In the absence of any signal at this energy, the $[\tan\beta, M_A]$ plane can be entirely closed for any $\tan\beta$ value and a pseudoscalar mass below $M_A \approx 500$ GeV. Additional and complementary searches can also be done in the charged Higgs case in channels that have not been studied so far such as $H^+ \to Wh$ but we did not analyze this issue in detail.

Hence, all channels that have been considered for the SM Higgs boson in the high mass range, plus some processes that have been considered for other new physics searches, can be recycled for the search of the heavier MSSM Higgs bosons in the low $\tan\beta$ regime. For instance, many of these MSSM Higgs processes could benefit from the current searches of multi–lepton events with missing energy in SUSY theories. As in all channels we have W, Z and additional h bosons in the final states, multileptons and missing energy are present in most of the topologies. One could then use the direct searches for SUSY particles such as charginos and neutralinos to probe also the MSSM heavier Higgs states.

All this promises a very nice and exciting program for Higgs searches at the LHC in both the present and future runs. One could then cover the entire MSSM parameter space: from above (at high $\tan\beta$) by improving the $H/A \to \tau\tau$ searches but also from below (at low $\tan\beta$) by using the $WW, ZZ, tt, ..$ searches. The coverage of the $[\tan\beta, M_A]$ plane will be done in a model independent way, with no assumption on M_S and possibly on any other SUSY parameter[13]. The indirect information from the lighter Higgs mass will be included as well as the information from the Higgs couplings, as the sensitivity regions cover also that which are excluded from the measurement of the h properties at the LHC.

One can of course use these channels in other extensions of the SM. An example would be SUSY extensions beyond the MSSM where M_h can be made large enough without having large M_S values; this is the case of the NMSSM where the maximal M_h value can be obtained at $\tan\beta \approx 2$ [89]. Another example would be a non–SUSY two–Higgs doublet model where there is more freedom in the parameters space and all channels analyzed here and even some more could be relevant; discussions along these lines have already started [82, 90]). The numerous search channels discussed in this paper might allow to probe in a more comprehensive manner the extended parameter space of these models.

Acknowledgements: AD thanks the CERN theory division for the kind hospitality offered to him. This work is supported by the ERC Advanced Grant Higgs@LHC.

[13]This approach is orthogonal to that of Ref. [32] in which specific benchmark scenarios with fixed SUSY parameters (which might need to be updated soon) are proposed. We note that for all the proposed benchmarks scenarios [32], the SUSY scale is fixed to $M_S = 1$ or 1.5 TeV which excludes the low (and possibly intermediate) $\tan\beta$ regime and, hence, the possibility of discussing the processes analysed here.

References

[1] The ATLAS collaboration, Phys. Lett. B716 (2012) 1; the CMS collaboration, Phys. Lett. B716 (2012) 30.

[2] P. Higgs, Phys. Lett. 12 (1964) 132; F. Englert and R. Brout, Phys. Rev. Lett. 13 (1964) 321; G. Guralnik, C. Hagen and T. Kibble, Phys. Rev. Lett. 13 (1964) 585; P. Higgs. Phys. Rev. 145 (1966) 1156.

[3] J. Gunion, H. Haber, G. Kane and S. Dawson, "The Higgs Hunter's Guide", Reading 1990.

[4] A. Djouadi, Phys. Rept. 457 (2008) 1, [arXiv:hep-ph/0503172].

[5] H. Haber and G. Kane, Phys. Rep. 117 (1985) 75; S. Martin, hep-ph/9709356; M. Drees, R. Godbole and P. Roy, *Theory and phenomenology of sparticles*, World Scientific, 2005.

[6] A. Djouadi et al. (MSSM Working Group), hep-ph/9901246.

[7] A. Djouadi, Phys. Rept. 459 (2008) 1, [arXiv:hep-ph/0503173].

[8] M. Carena and H. Haber, Prog. Part. Nucl. Phys. 50 (2003) 63; S. Heinemeyer, W. Hollik and G. Weiglein, Phys. Rept. 425 (2006) 265; B.C. Allanach et al., JHEP 0409 (2004) 044.

[9] A. Arbey et al., Phys. Lett. B708 (2012) 162.

[10] See the talks given by the members of the ATLAS and CMS collaborations at the XLVIIIth "Rencontres de Moriond", 2-16 March 2013, La Thuile, Italy.

[11] See for instance, H.E. Haber, CERN-TH/95-109 and hep-ph/9505240.

[12] See e.g. R. Barbieri and G.F. Giudice, Nucl. Phys. B306 (1988) 63.

[13] The LEP collaborations, Eur.Phys.J. C47 (2006) 547.

[14] N. Arkani-Hamed and S. Dimopoulos, JHEP 0506 (2005) 073; G.F. Giudice and A. Romanino, Nucl. Phys. B699 (2004) 65; J.D. Wells, Phys. Rev. D71 (2005) 015013.

[15] See e.g. L.J. Hall and Y. Nomura, JHEP 1003 (2010) 076.

[16] J. R. Ellis et al., Nucl. Phys. B 652 (2003) 259; H. Baer et al., Phys. Rev. D 71 (2005) 095008; J. R. Ellis, K. A. Olive and P. Sandick, Phys. Rev. D 78 (2008) 075012; L. Roszkowski et al., Phys. Rev. D 83 (2011) 015014. For a recent account, see e.g. S.S. AbdusSalam et al., Eur. Phys. J. C71 (2011) 1835.

[17] A. Delgado and G.F. Giudice, Phys. Lett. B627 (2005) 155; E. Arganda, J.L. Diaz-Cruz and A. Szynkman, arXiv:1211.0163 and arXiv:1301.0708.

[18] A. Djouadi, J.L. Kneur and G. Moultaka, Comput. Phys. Commun. 176 (2007) 426.

[19] H. Baer, F. Paige, S.. Protopopescu and X. Tata, hep-ph/0001086; B. Allanach, Comput. Phys. Commun. 143 (2002) 305; W. Porod, Comput. Phys. Commun. 153 (2003) 275.

[20] N. Bernal, A. Djouadi and P. Slavich, JHEP 0707 (2007) 016.

[21] E. Bagnaschi, N. Bernal, A. Djouadi, J. Quevillon and P. Slavich, in preparation.

[22] Y. Okada, M. Yamaguchi and T. Yanagida, Prog. Theor. Phys. 85 (1991) 1; J. Ellis, G. Ridolfi and F. Zwirner, Phys. Lett. B257 (1991) 83; H.E. Haber and R. Hempfling, Phys. Rev. Lett. 66 (1991) 1815.

[23] See, for instance, F. Zwirner, hep-ph/9203204.

[24] D. Pierce, J. Bagger, K. Matchev and R. Zhang, Nucl. Phys. B491 (1997) 3.

[25] M. Carena, J.R. Espinosa, M. Quiros and C.E. Wagner, Phys. Lett. B355 (1995) 209; H. Haber, R. Hempfling and A. Hoang, Z. Phys. C75 (1997) 539.

[26] G. Degrassi, P. Slavich, F. Zwirner, Nucl. Phys. B611 (2001) 403; A. Brignole, G.Degrassi, P. Slavich and F. Zwirner, Nucl. Phys. B631 (2002) 195; Nucl. Phys. B643 (2002) 79.

[27] S. Heinemeyer, W. Hollik and G. Weiglein, Phys. Rev. D58 (1998) 091701; Eur. Phys. J.C9 (1999) 343.

[28] P. Kant, R.V. Harlander, L. Mihaila and M. Steinhauser, JHEP 1008 (2010) 104.

[29] A. Arbey, M. Battaglia, A. Djouadi and F. Mahmoudi, JHEP 1209 (2012) 107.

[30] A. Arbey, M. Battaglia, A. Djouadi and F. Mahmoudi, Phys. Lett. B720 (2013) 153.

[31] M. Carena, S. Heinemeyer, C. Wagner and G. Weiglein, Eur. Phys. J. C26 (2003) 601.

[32] M. Carena et al., arXiv:1302.7033

[33] S. Heinemeyer, W. Hollik and G. Weiglein, Comp. Phys. Commun. 124 (2000) 76.

[34] J. Beringer (Particle Data Group) et al., Phys. Rev. D86 (2012) 010001.

[35] S. Alekhin, A. Djouadi and S. Moch, Phys. Lett. B716 (2012) 214.

[36] G. Giudice and A. Strumia, Nucl.Phys. B858 (2012) 63.

[37] J. Feng, K. Matchev and T. Moroi, Phys. Rev. Lett. 84 (2000) 2322; Phys. Rev. D61 (2000) 075005; J.L. Feng, arXiv:1302.6587 [hep-ph].

[38] See eg.g. D. Feldman, G. Kane, E. Kuflik and R. Lu, Phys. Lett. B704 (2011) 56; S. Akula, B. Altunkaynak, D. Feldman, Pran Nath and G. Peim, Phys. Rev. D85 (2012) 075001 B. Acharya, G. Kane and P. Kumar, Int. J. Mod. Phys. A27 (2012) 1230012; G. Kane, R. Lu and B. Zheng, Int. J. Mod.Phys. A28 (2013) 1330002.

[39] See e.g., M. Carena, D. Garcia, U. Nierste and C.E. Wagner, Nucl. Phys. B577 (2000) 88; D. Noth and M. Spira, Phys. Rev. Lett. 101 (2008) 181801.

[40] A. Djouadi, W. Kilian, M.M. Muhlleitner and P.M. Zerwas, Eur. Phys. J. C10 (1999) 27; Eur. Phys. J. C10 (1999) 45.

[41] E. Boos et al., Phys. Rev. D66 (2002) 055004; E. Boos, A. Djouadi and A. Nikitenko, Phys. Lett. B578 (2004) 384.

[42] J. Baglio and A. Djouadi, JHEP 1103 (2011) 055.

[43] J. Baglio and A. Djouadi, Phys. Lett. B699 (2011) 372; arXiv:1103.6247.

[44] S. Dittmaier et al. (LHC Higgs Working Group), arXiv:1101.0593 [hep-ph].

[45] D. Dicus and S. Willenbrock, Phys. Rev. D39 (1989) 751.

[46] M. Spira, A. Djouadi, D. Graudenz and P.M. Zerwas, Nucl. Phys. B453 (1995) 17.

[47] M. Spira, Fortschr. Phys. 46 (1998) 203; hep-ph/9510347.

[48] Michael Spira site: `http://mspira.home.cern.ch/ mspira/proglist.html`.

[49] J. Campbell, R. K. Ellis, F. Maltoni and S. Willenbrock, Phys. Rev. D67 (2003) 095002; F. Maltoni, Z. Sullivan and S. Willenbrock Phys. Rev. D67 (2003) 093005.

[50] R. Harlander and W. Kilgore, Phys. Rev. D68 (2003) 013001.

[51] R. Harlander, S. Liebler and H. Mantler, Comp. Phys. Comm. 184 (2013) 1605.

[52] S. Dittmaier, M. Krämer and M. Spira, Phys. Rev. D70 (2004) 074010; S. Dawson et al, Phys. Rev. D69 (2004) 074027.

[53] A. Arbey, M. Battaglia and F. Mahmoudi, arXiv:1303.7450.

[54] S. Dawson, A. Djouadi and M. Spira, Phys. Rev. Lett. 77 (1996) 16; R. Harlander and M. Steinhauser, JHEP 0409 (2004) 066, ibid. Phys. Rev. D68 (2003) 111701; M. Muhlleitner, H. Rzehak and M. Spira, JHEP 0904 (2009) 023.

[55] ATLAS Collaboration, ATLAS-CONF-2012-105 and ATLAS-CONF-2012-108; CMS Collaboration, arXiv:1301.0916 and arXiv:1212.6428.

[56] ATLAS Collaboration, ATLAS-CONF-2013-010 and arXiv:1211.6956; CMS Collaboration, CMS-HIG-12-011.

[57] CMS Collaboration, CMS-PAS-HIG-12-033.

[58] A.D. Martin, W. Strirling, R. Thorne and G. Watt, Eur. Phys. J. C63 (2009) 189.

[59] A. Djouadi, M. Spira and P.M. Zerwas, Phys. Lett. B264 (1991) 440; S. Dawson, Nucl. Phys. B359 (1991) 283; M. Spira et al., Phys. Lett. B318 (1993) 347.

[60] R.V. Harlander and W. Kilgore, Phys. Rev. Lett. 88 (2002) 201801; C. Anastasiou and K. Melnikov, Nucl. Phys. B646 (2002) 220; V. Ravindran, J. Smith and W.L. Van Neerven, Nucl. Phys. B665 (2003) 325; R. Harlander and W. Kilgore, JHEP 0210 (2002) 017.
S. Catani et al., JHEP 0307 (2003) 028.

[61] A. Bawa, C. Kim and A. Martin, Z. Phys. C47 (1990) 75; V. Barger, R. Phillips and D.P. Roy, Phys. Lett. B324 (1994) 236; S. Moretti and K. Odagiri, Phys. Rev. D55 (1997) 5627; J. Gunion, Phys. Lett. B322 (1994) 125; F. Borzumati, J.L. Kneur and N. Polonsky, Phys. Rev. D60 (1999) 115011.

[62] T. Plehn, Phys. Rev. D67 (2003) 014018.

[63] For a review, see: S. Moretti, Pramana 60 (2003) 369.

[64] A. Djouadi, J. Kalinowski and M. Spira, Comput. Phys. Commun. 108 (1998) 56. An update of the program with M. Muhlleitner in addition appeared in hep-ph/0609292.

[65] A. Djouadi, J. Kalinowski and P. Zerwas, Z. Phys. C70 (1996) 435; S. Moretti, J. Stirling, Phys. Lett. B347 (1995) 291; F. Borzumati and A. Djouadi, Phys. Lett. B549 (2002) 170.

[66] The ATLAS collaboration, ATLAS-CONF-2013-014.

[67] The CMS collaboration, CMS-PAS-HIG-13-001

[68] The ATLAS collaboration, ATLAS-CONF-2013-013.

[69] The CMS collaboration, CMS-PAS-HIG-13-002.

[70] The ATLAS collaboration, ATLAS-CONF-2013-030.

[71] The CMS collaboration, CMS-PAS-HIG-13-003.

[72] The ATLAS collaboration, ATLAS-CONF-2012-161.

[73] The CMS collaboration, CMS-PAS-HIG-12-044.

[74] The ATLAS collaboration, ATLAS-CONF-2012-094 and arXiv:1211.6956.

[75] The CMS collaboration, CMS-PAS-HIG-12-050.

[76] The ATLAS collaboration, ATLAS-CONF-2012-011 and arXiv:1204.2760.

[77] The CMS collaboration, CMS-HIG-11-019 and arXiv:1205.5736.

[78] A. Djouadi, arXiv:1208.3436; A. Djouadi and G. Moreau, arXiv:1303.6591.

[79] A. Djouadi, see talks given in e.g. "Rencontres de la Vallée d'Aoste", La Thuile, February 2013; "Discrete 2012", Lisbon, December 2012; CMS Exotic Higgs group meeting, CERN, February 2013; ATLAS MSSM Higgs group meeting, CERN, December 2012.

[80] See for instance L. Maiani and A.D. Polosa, Phys. Lett. B718 (2012) 465; M. Carena, P. Draper, T. Liu and C. Wagner, Phys. Rev. D84 (2011) 095010; N. Christensen, T. Han and S. Su, Phys. Rev. D85 (2012) 115018; J. Chang, K. Cheung, P. Tseng and T-C. Yuan, Phys.Rev. D87 (2013) 035008.

[81] The CMS collaboration, arXiv:1304.0213.

[82] The ATLAS collaboration, ATLAS-CONF-2013-027.

[83] The ATLAS collaboration, arXiv:1207.2409.

[84] The CMS collaboration, arXiv:1211.3338.

[85] T. Plehn, G.P. Salam and M. Spannowsky, Phys. Rev. Lett. 104 (2010) 111801.

[86] J. Butterworth, A. Davison, M. Rubin and G. Salam, Phys. Rev. Lett. 100 (2008) 242001.

[87] J. Baglio et al., arXiv:1212.5581 [hep-ph].

[88] The ATLAS collaboration, ATLAS-CONF-2011-094 and arXiv:1302.3694.

[89] U. Ellwanger, C. Hugonie and A.M. Teixeira, Phys. Rept. 496 (2010) 1; M. Maniatis, Int.J.Mod.Phys. A25 (2010) 3505; A. Djouadi et al., JHEP 0807 (2008) 002. For recent discussions, see: G. Bélanger et al., JHEP 1301 (2013) 069; S. King, M. Muhlleitner and R. Nevzorov, Nucl.Phys. B860 (2012) 207.

[90] G. Branco et al., Phys. Rept. 516 (2012) 1. For recent discussions, see: Y. Bai et al., arXiv:1210.4922; S. Chang et al., arXiv:1210.3439; A. Drozd et al., arXiv: 1211.3580; J. Chang et al., arXiv:1211.3849; B. Grinstein and P. Uttayarat, arXiv:1304.0028.